J. Cent. South Univ. (2019) 26: 3436−3456
DOI: https://doi.org/10.1007/s11771-019-4265-6

Springer

Depositional conditions and modeling of Triassic Oil shale in southern Ordos Basin using geochemical records

LI De-lu(李得路)[1, 2, 3], LI Rong-xi(李荣西)[4], TAN Cheng-qian(谭成仟)[5], ZHAO Di(赵迪)[4], LIU Fu-tian(刘福田)[4], ZHAO Bang-sheng(赵帮胜)[4]

1. Shaanxi Provincial Key Laboratory of Geological Support for Coal Green Exploitation, Xi'an University of Science and Technology, Xi'an 710054, China;
2. Geological Research Institute for Coal Green Mining, Xi'an University of Science and Technology, Xi'an 710054, China;
3. College of Geology and Environment, Xi'an University of Science and Technology, Xi'an 710054, China;
4. School of Earth Sciences and Resources, Chang'an University, Xi'an 710054, China;
5. School of Earth Sciences and Engineering, Xi'an Shiyou University, Xi'an 710065, China

Abstract: Based on the element geochemistry and biomarkers of the oil shale from the Chang 7 sub-unit in the southern Ordos Basin, the depositional conditions and organic source of the oil shale are discussed. Biomarkers analyses show that the oil shale has a homologous organic matter source, with a mix of plankton and advanced plants. U/Th and V/Ni ratios suggest that the redox condition is dominated by a reducing condition, and the degree of anoxia in the Tongchuan area is higher than that of the Xunyi area. Sr/Ba ratios illustrate that the oil shale is deposited in fresh water and the paleosalinity in the Tongchuan area is slightly higher. Fe/Ti ratios imply that the Tongchuan area underwent obvious hydrothermal fluid activities. Sr/Cu ratios show warm and humid paleoclimate in both areas. As assessed by $(La/Yb)_{NASC}$, the deposition rate in the Tongchuan area is relatively lower. Fe/Co and Th/U ratios suggest that the paleo-water-depth in the Tongchuan area is deeper. The source rock could have the advance plants source, which must have close relationship with the Qinling orogeny. Comparing the paleoenvironment, the Tongchuan area has better depositional conditions, and is the key oil shale exploration area in the southern Ordos Basin.

Key words: oil shale; geochemistry; depositional model; Chang 7; Ordos Basin

Cite this article as: LI De-lu, LI Rong-xi, TAN Cheng-qian, ZHAO Di, LIU Fu-tian, ZHAO Bang-sheng. Depositional conditions and modeling of Triassic Oil shale in southern Ordos Basin using geochemical records [J]. Journal of Central South University, 2019, 26(12): 3436−3456. DOI: https://doi.org/10.1007/s11771-019-4265-6.

1 Introduction

Oil shale is a type of fine grained sediment with high organic matter; it can release shale oil after combustion [1−3]. Due to the dwindling of conventional oil resources, oil shale, as an unconventional alternative resource, has received unprecedented attention [4−8]. The most studied oil shale in the world is the lacustrine oil shale of the Green River Basin in the United States, which has the largest amount of resources [1, 9, 10]. Chinese oil shale is primarily distributed in the Songliao Basin and Ordos Basin; the oil shale from the Triassic Chang 7 sub-unit in the southern Ordos Basin is characterized by shallow burial depth, extensive distribution, and relatively high oil yield [1, 11−13].

Foundation item: Projects(41173055, 41772118) supported by the National Natural Science Foundation of China
Received date: 2018-12-18; **Accepted date:** 2019-02-27
Corresponding author: LI De-lu, PhD, Lecturer; Tel: +86-18402990271; E-mail: lidelu322@126.com; ORCID: 0000-0003-2211-6840

Studies indicate that the organic matter of oil shale from the Chang 7 sub-unit is dominated by Type I and II, and the origin of the organic matter is primarily algae, with low maturity [14, 15]. After analysis of a large data set obtained from boreholes and a geology survey, LUO et al [16] suggested that the thickness of the oil shale varies from 10 to 40 m. The oil shale is deposited in fresh water under 150 m maximum depth [17]. SUN et al [18] considered that lake flooding, together with anoxic events, volcanic movements, and turbidity events have important effects on enrichment, preservation, abundance, and the type of organic matter in oil shale. After interpretation of a large number of well logs, DENG et al [19] forecasted that the Tongchuan and Xunyi areas in the southern Ordos Basin have favorable potential for oil shale development. The sedimentary environment affects the elemental geochemical behavior of sedimentary rocks, and vice versa; elemental geochemical characteristics can also reflect the ancient environment of the sedimentary period [20−22]. Elemental geochemistry is an effective means of paleo-environment reconstruction. The redox condition, salinity, hydrothermal fluid activities, climate, sedimentary rate, and water depth can be recovered by the element ratios and their related calculation, semi-quantitatively or quantitatively [3, 23−25]. These values have a close relationship with enrichment and preservation of organic matter [26, 27]. Compared to qualitative analysis of the paleo-environment by rock combinations and organic geochemistry, elemental geochemical recovery is more accurate.

In addition to being used for oil and source rock correlation, biomarkers have implications for the source of organic matter in source rocks [3, 28−30]. YANDOKA et al [31] suggested that regular sterane (C_{27}, C_{28} and C_{29}) can indicate different sources of organic matter, and found that the organic matter of Cretaceous sediments in the Yola Sub-basin was dominated by planktonic/ bacterial matter. HAKIMI et al [4] considered the relative amount regular sterane, and found that the organic matter of Mesozoic oil shale in central Jordan was primarily composed of plankton/algal matter and microorganisms. Thus, understanding of the source of organic matter can be achieved through analysis of the regular sterane in biomarkers.

Up to now, in most lacustrine basins, the organic matter source of the superb source rock often originates from inferior algal organism. The oil shale from Green River Formation in American has been verified that the lower biological debris contribute to the organic matter in the oil shale [32, 33]. The organic matter type of the fresh water oil shale in Huadian in northeastern China is dominated by Type I, reflecting that organic matter source is mainly inferior algal organism [34]. The Permian oil shale of Junggar Basin in western China was formed in a closed freshwater lake with the lower aquatic organisms as the main organic matter source [35, 36]. It is worth noting that the above lacustrine oil shales are almost deposited in a relatively stable sedimentary environment. The researches on the oil shale in complex tectonic environment are still insufficient.

Oil shale outcrops and boreholes from the Chang 7 sub-unit in the Tongchuan and Xunyi areas have similar physical properties with a huge amount of resources, over 14159.04×10^8 t [13]. According to sedimentary facies, the Tongchuan and Xunyi areas are all located in semi-deep to deep lake, facilitating oil shale formation [37]. However, the average thickness and oil yield in Tongchuan area are around 30 m and 5%−10% [22]. While, the thickness and oil yield of the oil shale in Xunyi area are obviously smaller than that in Tongchuan area. This is likely to be associated with the depositional conditions. Moreover, the total organic matter of the oil shale from the Tongchuan area is slightly higher than that from the Xunyi area [13,15], and complex geological events happening in the southern Ordos Basin during oil shale sedimentation are likely to have a different effect on depositional conditions [3, 38, 39]. Therefore, it is necessary to investigate the depositional conditions of the two areas in southern Ordos Basin to find out the reasons for the differences in the thickness, oil yield and total organic matter. This can provide theoretical direction for further oil shale exploration in the southern Ordos Basin.

In this work, oil shale samples from the Tongchuan and Xunyi areas in the southern Ordos Basin are analyzed with regard to major elements, trace elements, and rare earth elements (REEs), and gas chromatography-mass spectromete (GC-MS) is performed. The organic matter source of the oil shale is discussed and the paleo-environment of the oil shale in these two areas is compared. Finally, a depositional model of oil shale from the Chang 7 sub-unit is proposed.

2 Geological setting

Located in midwestern China, the Ordos Basin is a superimposed basin with stable deposition and multiple sedimentary cycles [30, 40, 41]. Before the Carboniferous-Permian period, the basin belonged to the marine basin of the North China Block [39], and then gradually departed from the North China Block and evolved into a large inland sedimentary basin [40, 41]. In the Early Cretaceous, the whole basin uplifted and underwent later reformation. According to the present tectonic characteristics and evolutionary history, the basin is divided into six first-order tectonic units, including the Weibei Uplift, Yishan Slope, Yimeng Uplift, Jinxi Flexure Zone, Tianhuan Depression, and Western Thrusted Zone (Figure 1(a)). The Triassic Yanchang Formation primarily developed delta and lake facies, and went through an integrated occurrence-extinction period, depositing a set of progradation-aggradation-retrogradation stratum, with a thickness of 1000−1300 m [41−43]. According to the sedimentary cycles and rock assemblages, the Yanchang Formation is divided into 10 sub-units [44], reflecting a whole transgressive–regressive lacustrine cycle [39, 41]. In particular, during the initial stage of the Chang 7 period, the lake reached its largest scale, and together with tectonic

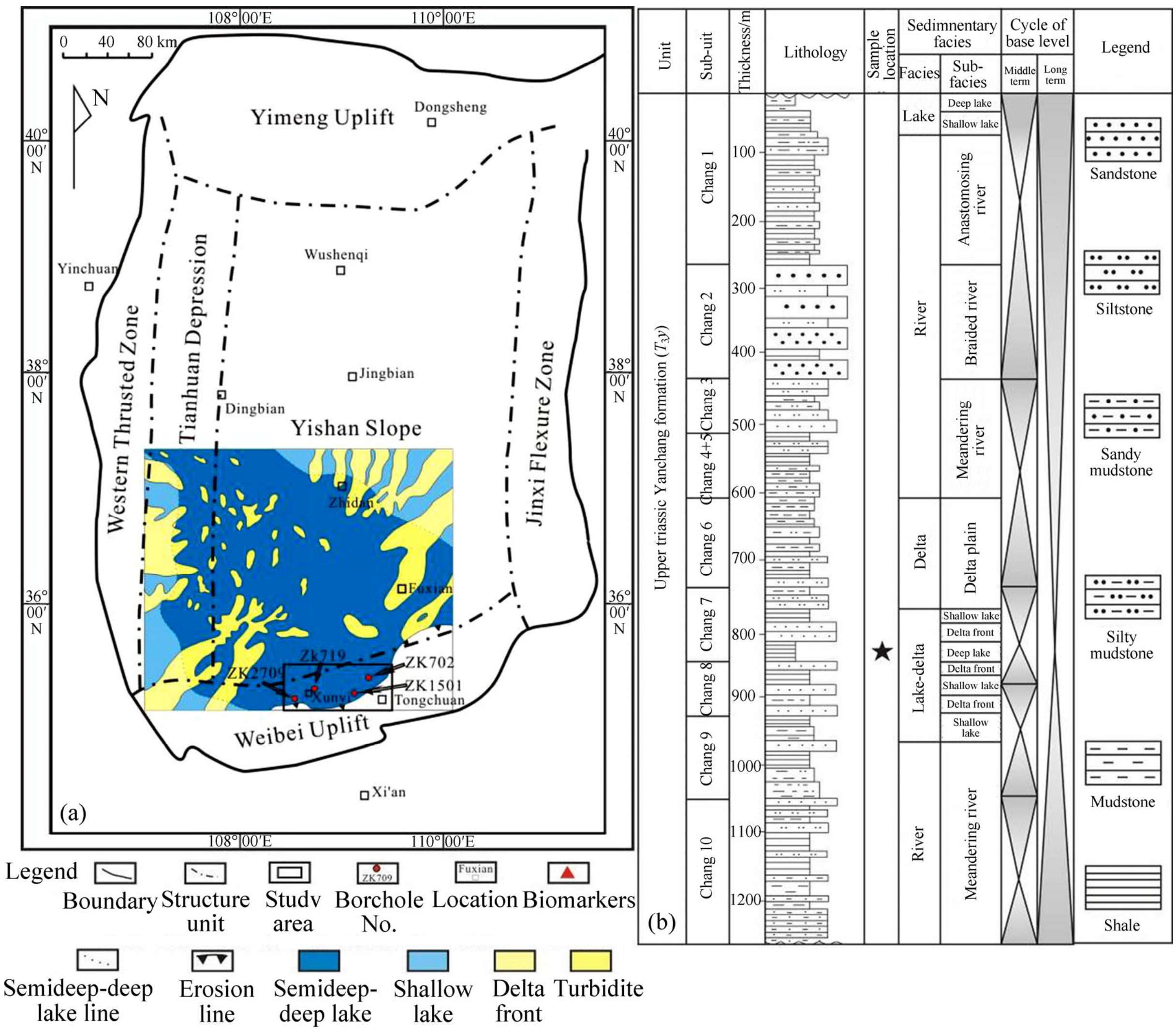

Figure 1 Geological map of Ordos Basin (modified after LI et al [22]), sedimentary facies of southern Ordos Basin (modified after YANG et al [37]), and location of study area, showing that study area is primarily located in the Weibei Uplift, and the depositional sub-facies is semi-deep to deep lake (a) and stratigraphic column of Upper Triassic Yanchang Formation in study area (modified after LI et al [22]), showing that whole Yanchang Formation represents evolutionary process of the lake, from start to end. Chang 7 period comprises the largest lake with premium oil shale (b)

orogenies and paroxysmal eruption in the south [22, 39] and formed a high quality of oil shale characterized by a huge thickness and high organic content. This was named the Zhangjiatan Oil Shale [45, 46]; it is located at the bottom of the Chang 7 sub-unit, and contributes to the entire Mesozoic oil reservoirs in the Ordos Basin [19, 47, 48].

The study area is primarily located in the Weibei Uplift of the southern Ordos Basin. Due to the Indosinian orogeny and the Yanshan Orogeny, the study area underwent unbalanced uplift, and missed the upper stratums in the Yanchang Formation with the current stratum of Chang 10−Chang 6. Previous studies have indicated that the southern Ordos Basin is the depocenter of the lake and the sub-facies is semi-deep to deep lake during Chang 7 period [22, 37] (Figure 1(a)). The bottom of the Chang 7 sub-unit primarily developed oil shale, shale, mudstone, and silty mudstone (Figure 1(b)).

3 Sampling and analytical methods

A total of 26 oil shale samples were collected in the Tongchuan and Xunyi areas and the oil shale samples were all from the bottom of Chang 7 sub-unit. Twenty of them were selected from 4 boreholes scattered in southern Ordos Basin and sent to analyze major elements, trace elements and rare earth elements (Figure 2). Six of them were analyzed by GC-MS, in which three were collected from Yishicun profile in the Tongchuan area and the other three were collected from three well drillings in the Xunyi area (Figure 1(a)).

The samples for element analysis were all powdered to less than 75 μm, using X-ray fluorescence spectrometry (XRF) for major elements and inductively-coupled plasma mass spectrometer (ICP-MS) for trace elements and rare earth elements. For XRF, the ashed samples were first sent to an open muffle furnace with the mounting temperature of 950 °C and then were dissolved with $HClO_4$ and HF. The operation was conducted by AA-6800 atomic absorption spectroscopy and UV-2600 ultraviolet-visible spectrophotometer. For ICP-MS, the ashed samples were digested in microwave furnace by an $HF+HNO_3$ mixture liquid in Teflon bombs at 190 °C for 48 h. The operation was conducted by Perkin Elmer SciexElan 6000. The analytical procedures followed Chinese National Standard GB/T14506.1-14-2010 [49] and GB/T14506.30-2010 [50], respectively. The analytical error was within 1%. The analyses were performed at the Analytical Center, No.203 Research Institute of Nuclear Industry.

For gas chromatography-mass spectrometry (GC-MS) analyses, samples were extracted with chloroform ($CHCl_3$) for 72 h after being powdered under 80 mesh and silica gel, together with alumina column, which was used to separate group composition. Saturated hydrocarbon, aromatic and nonhydrocarbon were obtained with n-Hexane, benzene and ethanol as solvent. Corresponding biomarkers were performed on an Agilent 6890GC/5975i MS with a 60 m×0.25 mm×0.25 μm HP-5MS fused silica capillary column under condition of 26 °C and 50% relative humidity (70 eV ionization voltage, 100 mA filament emission current, 150−250 °C interface temperature), with He as the carrier gas (30 m×0.32 mm). The gas was boosted at the rate of 1.0 mL/min and the start temperature of the oven is 50 °C. Then the oven was hearted to 310 °C at the rate of 20/min after 1 min, then held at 310 °C for 25 min. Testing standard was followed by GB/T 18606-2001 [51]. The experiments were conducted at Key Laboratory of Exploration Technologies for Oil and Gas Resources, Ministry of Education, Yangtze University, China.

4 Geochemistry characteristics

4.1 Elements geochemistry

The results of the major elements analysis of the oil shale samples are listed in Table 1. The concentration of SiO_2 (36.42 wt%−64.70 wt%) comprised almost half of the total concentration of major elements, and the concentrations of Al_2O_3 (10.69 wt%−20.15 wt%) and TFe_2O_3 (3.61 wt%−11.27 wt%) were also relatively high. The content of the rest of the major elements was very low, with averages of less than 5%. The element Si is enriched in oil shale samples, indicating that quartz is likely to be present (Figure 3(a)). This is in accordance with XRD analysis [22]. The elements Al and Ti are relatively stable and can be used to judge the parent rock type because of the low solubility of their oxides and hydroxides [52]. The

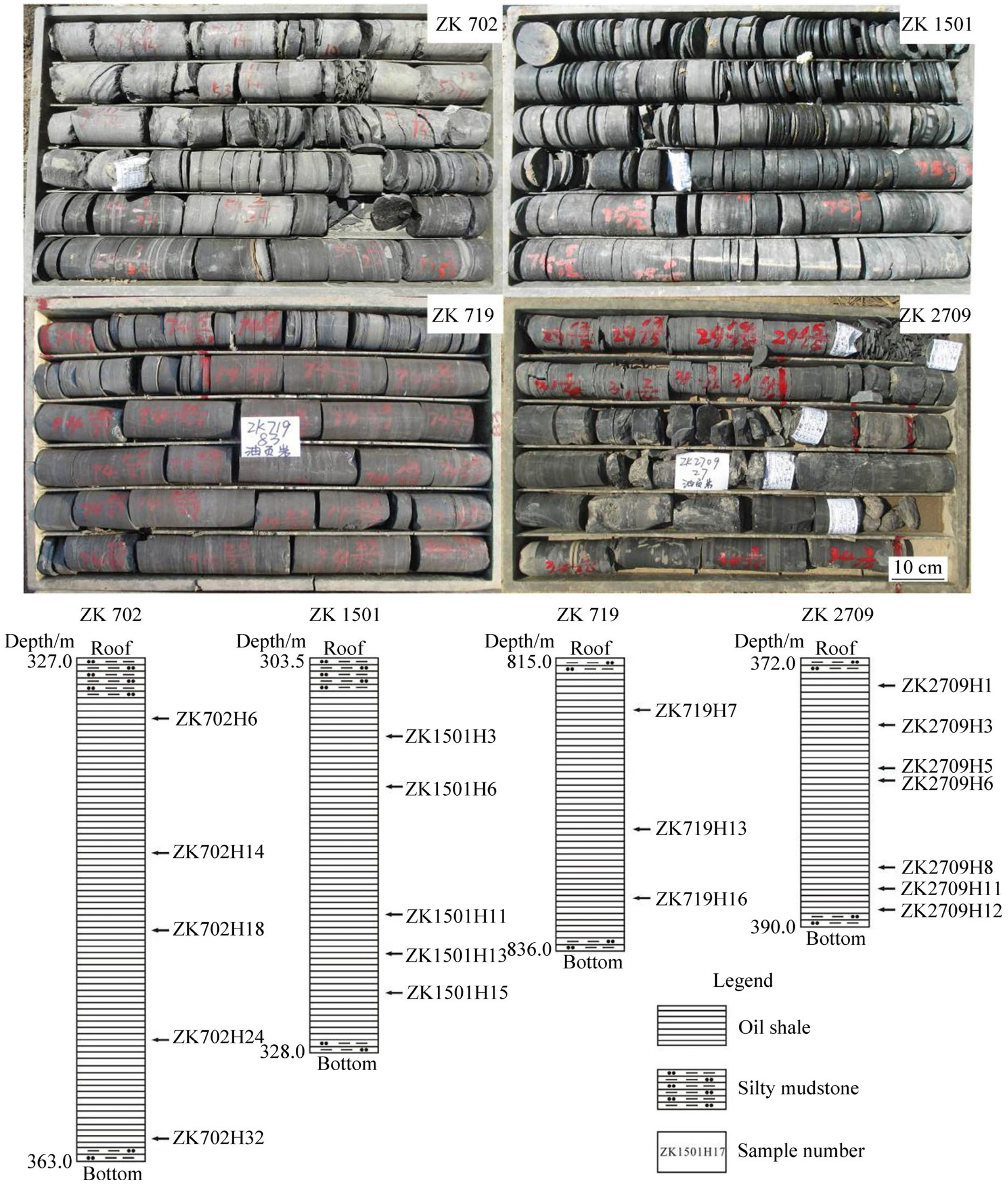

Figure 2 Photos (a) and sketches (b) of oil shale sections from four boreholes and sampling locations in the Chang 7 sub-unit. The length of sample boxes is 1 m and the diameter of the core columns is 7 cm. The top of the oil shale section is located in the upper left corner and the bottom is in the lower right corner. Oil shale portions are layered with lamina tuff and massive microstructures

Al_2O_3/TiO_2 ratio is regarded as very contiguous to that of the parent rocks. Al_2O_3/TiO_2 ratios ranging in 3−8, 8−21 and 21−70 are indicative of mafic igneous rocks, intermediate rocks, and felsic igneous rocks, respectively [53]. The Al_2O_3/TiO_2 ratios of the oil shale samples varied from 21.76 to 46.69, indicating that the parent rock of the oil shale is felsic igneous rock (Figure 3). The Al_2O_3/TiO_2 ratios of the oil shale samples in the Tongchuan area (28.8−46.7, averaging 34.5) were slightly higher than those of the Xunyi area (21.7−33.3, averaging 27.3); this may be due to the paleo-environment. Si/(Si+Al+Fe) is a reflection of distance from the terrigenous provenance, and decreases with

Table 1 Concentrations of major elements and associated geochemical parameters of oil shale samples from Chang 7 sub-unit

Location	Samples No.	Mass fraction/%											
		SiO_2	Al_2O_3	TFe_2O_3	MgO	CaO	Na_2O	K_2O	P_2O_5	MnO	TiO_2	Al_2O_3/TiO_2	Si/(Si+Al+Fe)
Xunyi area	ZK2709H1	53.80	20.15	7.28	2.08	0.94	1.17	3.02	0.23	0.23	0.77	26.17	0.61
	ZK2709H3	44.44	14.15	8.03	1.71	1.59	1.29	2.53	0.39	0.19	0.51	27.75	0.61
	ZK2709H5	64.70	14.00	3.61	1.19	1.24	1.73	2.43	0.12	0.14	0.42	33.33	0.75
	ZK2709H6	46.51	13.44	7.46	1.76	2.09	1.39	2.23	0.38	0.19	0.52	25.85	0.64
	ZK2709H8	50.17	15.92	7.61	2.01	1.17	1.14	2.80	0.27	0.16	0.63	25.27	0.63
	ZK2709H11	49.72	16.53	7.54	2.06	1.02	1.03	2.74	0.23	0.13	0.61	27.10	0.62
	ZK2709H12	62.40	16.97	5.80	2.09	0.39	2.05	3.10	0.13	0.06	0.78	21.76	0.69
	ZK719H7	52.60	17.95	7.16	2.39	1.39	0.78	2.18	0.15	0.14	0.64	28.05	0.63
	ZK719H13	47.03	17.07	6.21	1.74	0.73	0.76	2.54	0.24	0.15	0.54	31.61	0.62
	ZK719H16	56.23	18.72	6.14	2.08	1.92	0.82	2.22	0.14	0.09	0.73	25.64	0.65
Tongchuan area	ZK1501H3	45.36	11.45	9.57	1.06	1.62	1.45	2.12	0.36	0.11	0.39	29.36	0.62
	ZK1501H6	36.42	11.37	11.27	1.45	2.19	0.74	1.90	0.26	0.08	0.35	32.49	0.55
	ZK1501H11	43.58	12.96	9.87	1.16	2.36	1.43	2.03	0.41	0.21	0.45	28.80	0.60
	ZK1501H13	56.52	14.20	5.48	2.31	3.48	1.92	2.09	0.23	0.10	0.42	33.81	0.70
	ZK1501H15	48.09	14.00	7.97	1.22	1.98	1.30	2.36	0.46	0.25	0.39	35.90	0.63
	ZK702H6	55.73	13.54	6.95	0.75	0.42	0.98	3.61	0.24	0.09	0.29	46.69	0.68
	ZK702H14	40.61	13.37	10.52	0.97	0.97	0.91	2.25	0.28	0.05	0.40	33.43	0.57
	ZK702H18	46.90	10.69	9.48	0.86	1.61	1.30	1.85	0.45	0.06	0.36	29.69	0.64
	ZK702H24	43.33	12.50	8.85	0.98	1.67	1.49	1.49	0.35	0.07	0.33	37.88	0.61
	ZK702H32	44.26	12.66	9.62	0.93	1.25	1.00	2.37	0.29	0.09	0.34	37.24	0.61
Xunyi area(average)		52.76	16.49	6.68	1.91	1.25	1.22	2.58	0.23	0.15	0.62	27.25	0.65
Tongchuan area(average)		46.08	12.67	8.96	1.17	1.76	1.25	2.21	0.33	0.11	0.37	34.53	0.62

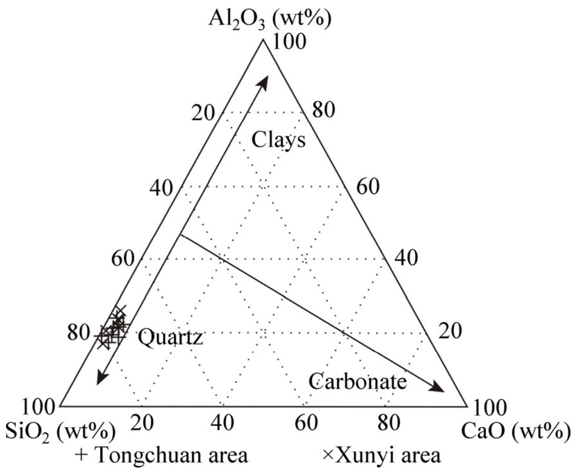

Figure 3 Rock type ternary diagram, showing relative proportions of major elements SiO_2(quartz), Al_2O_3(clays), and CaO(carbonates) in oil shale samples. This shows that the Si concentration in oil shale is relatively high and quartz is dominant mineral. The base map is from LI et al [26]

increasing distance [54]. The average Si/(Si+Al+Fe) ratios of the oil shale samples in the Tongchuan (0.65) and Xunyi areas (0.62) were relatively small, with little variability, suggesting that the oil shale was formed near the terrigenous provenance.

The trace element contents of the oil shale samples are presented in Table 2. Compared with the upper continental crust (UCC), Cu and U were enriched in oil shale samples (Figure 4), and enrichment factors (EF, F_e) (F_e=X_{samles}/X_{ucc}) of Cu and U of oil shale samples in the Tongchuan area (Cu: 1.98−6.00, average 5.01; U: 7.14−24.36, average 17.87) were higher than in the Xunyi area (Cu: 1.25−3.90, average 2.30; U: 1.05−7.71, average 3.60) (Figure 4 and Table 3). Sr, Ba, V, Th, Co, Ni, and Sc of the oil shale samples in the two areas show little difference. The element Cu is often associated with organisms, and the enrichment of Cu can represent the prosperity of living matter in a lake [56]. In an oxidation state, the element U usually exists in the +6 valence state, and is inclined to dilute, while in a reducing state, it is poorly soluble in water and tends to gather in the

Table 2 Trace elements contents of samples and corresponding UCC values of oil shale samples from Chang 7 sub-unit ($\times10^{-6}$)

Location	Samples No.	Sr	Ba	V	Cu	Th	U	Co	Ni	Sc
Xunyi area	ZK2709H1	160.50	513.60	135.00	41.00	17.60	4.21	15.90	37.00	10.80
	ZK2709H3	192.40	649.50	189.50	97.50	13.10	17.70	17.80	36.80	12.70
	ZK2709H5	236.10	680.40	69.10	31.20	16.60	6.41	7.93	20.10	13.90
	ZK2709H6	182.00	612.00	179.00	95.90	12.00	21.60	17.50	36.90	16.50
	ZK2709H8	177.70	662.00	170.00	64.20	14.00	12.70	17.10	36.70	13.10
	ZK2709H11	159.30	692.70	153.00	66.60	14.40	12.40	18.30	40.70	10.10
	ZK2709H12	245.50	635.40	116.10	40.10	12.10	2.94	15.80	41.00	13.20
	ZK719H7	133.30	486.20	158.10	42.40	14.50	5.90	14.80	33.00	16.90
	ZK719H13	155.40	584.00	196.30	53.20	15.00	14.00	15.50	37.30	12.50
	ZK719H16	205.00	540.00	133.00	43.00	14.60	3.07	16.70	34.00	11.60
Tongchuan area	ZK1501H3	185.00	562.40	255.50	139.30	15.80	68.20	15.80	27.70	9.10
	ZK1501H6	151.70	438.50	286.70	150.10	12.60	61.70	18.90	31.20	18.70
	ZK1501H11	438.80	765.10	299.70	141.90	9.96	51.10	17.70	30.00	16.20
	ZK1501H13	436.80	631.70	114.90	49.40	19.60	20.00	12.00	17.40	11.10
	ZK1501H15	425.00	849.80	249.20	123.10	15.10	47.30	17.40	31.00	14.50
	ZK702H6	110.40	380.90	123.80	90.30	22.20	28.50	13.30	22.00	16.60
	ZK702H14	162.00	515.70	282.80	139.20	14.90	54.10	21.60	34.20	16.00
	ZK702H18	229.80	463.40	235.30	144.50	10.80	61.30	15.10	29.10	16.00
	ZK702H24	384.90	774.60	305.90	142.10	9.56	61.10	14.60	26.90	14.40
	ZK702H32	328.20	792.60	316.80	132.30	12.70	47.00	14.70	28.30	16.90
Xunyi area(average)		184.72	605.58	149.91	57.51	14.39	10.09	15.73	35.35	13.13
Tongchuan area(average)		285.26	617.47	247.06	125.22	14.32	50.03	16.11	27.78	14.95
UCC[a]		350	550	107	25	10.7	2.8	17	44	13.6

[a] Cited from MCLENNAN [55]

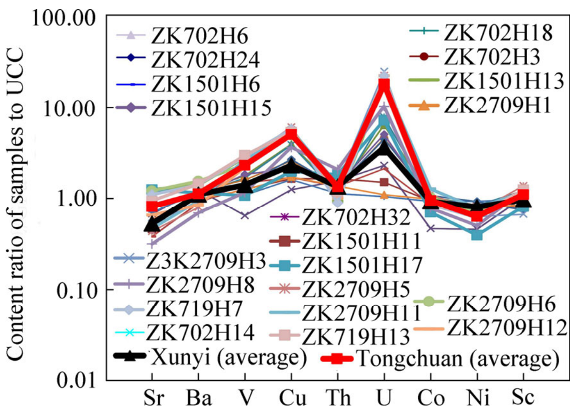

Figure 4 Spider diagram of trace elements of oil shale samples, indicating that oil shale from Tongchuan area is more enriched with U, Cu, and V elements, as compared to Xunyi area, which is likely related to depositional environment

form of the +4 valence state. Therefore, the extremely concentrated types of Cu and U are closely associated with high abundance of organic matter and a reducing condition [57, 58]. Therefore, the difference in Cu and U concentration is closely related with paleo-productivity and paleo-redox conditions.

The concentrations of rare earth elements in the oil shale samples are shown in Table 4. The total average content of rare earth elements (∑REE) of oil shale samples in the Tongchuan area (160.1 μg/g) is less than that in the Xunyi area (192.4 μg/g). The light rare earth elements (∑LREE) and heavy rare earth elements (∑HREE) of the oil shale samples in the Tongchuan area (∑LREE: 123.9−180.7 μg/g, averaging 143.6 μg/g; ∑HREE: 14.23−25.65 μg/g, averaging 16.52 μg/g) are mostly lower than those in the Xunyi area (∑LREE: 142.6−207.9 μg/g, averaging 175.2 μg/g; ∑HREE: 15.36−20.79 μg/g, averaging 17.17 μg/g). Moreover, the ∑LREE/∑HREE (L/H) of oil shale

Table 3 Enrichment factors of trace elements of oil shale samples from Chang 7 sub-unit

Location	Samples No.	Sr	Ba	V	Cu	Th	U	Co	Ni	Sc
Xunyi area	ZK2709H1	0.46	0.93	1.26	1.64	1.65	1.50	0.94	0.84	0.79
	ZK2709H3	0.55	1.18	1.77	3.90	1.22	6.32	1.05	0.84	0.93
	ZK2709H5	0.68	1.24	0.65	1.25	1.55	2.29	0.47	0.46	1.02
	ZK2709H6	0.52	1.11	1.67	3.84	1.12	7.71	1.03	0.84	1.21
	ZK2709H8	0.51	1.20	1.59	2.57	1.31	4.54	1.01	0.83	0.96
	ZK2709H11	0.46	1.26	1.43	2.66	1.35	4.43	1.08	0.93	0.74
	ZK2709H12	0.70	1.16	1.09	1.60	1.13	1.05	0.93	0.93	0.97
	ZK719H7	0.38	0.88	1.48	1.70	1.36	2.11	0.87	0.75	1.24
	ZK719H13	0.44	1.06	1.84	2.13	1.40	5.00	0.91	0.85	0.92
	ZK719H16	0.59	0.98	1.24	1.72	1.36	1.10	0.98	0.77	0.85
Tongchuan area	ZK1501H3	0.53	1.02	2.39	5.57	1.48	24.36	0.93	0.63	0.67
	ZK1501H6	0.43	0.80	2.68	6.00	1.18	22.04	1.11	0.71	1.38
	ZK1501H11	1.25	1.39	2.80	5.68	0.93	18.25	1.04	0.68	1.19
	ZK1501H13	1.25	1.15	1.07	1.98	1.83	7.14	0.71	0.40	0.82
	ZK1501H15	1.21	1.55	2.33	4.92	1.41	16.89	1.02	0.71	1.07
	ZK702H6	0.32	0.69	1.16	3.61	2.08	10.18	0.78	0.50	1.22
	ZK702H14	0.46	0.94	2.64	5.57	1.39	19.32	1.27	0.78	1.18
	ZK702H18	0.66	0.84	2.20	5.78	1.01	21.89	0.89	0.66	1.18
	ZK702H24	1.10	1.41	2.86	5.68	0.89	21.82	0.86	0.61	1.06
	ZK702H32	0.94	1.44	2.96	5.29	1.19	16.79	0.87	0.64	1.24
Xunyi area(average)		0.53	1.10	1.40	2.30	1.35	3.61	0.93	0.80	0.97
Tongchuan area(average)		0.82	1.12	2.31	5.01	1.34	17.87	0.95	0.63	1.10

Note: Enrichment factor=$X_{samples}/X_{ucc}$.

samples in the Tongchuan area (7.05−10.15, averaging 8.82) is lower than that in the Xunyi area (9.09−11.71, averaging 10.21).

Eu anomaly (δ_{Eu}) is the result of the differentiation of elements, and can reflect the parent rock properties [21, 24]. δ_{Eu} is regarded as a positive anomaly and negative anomaly when >1.05 and <0.95, respectively. Upper crustal rocks are normally characterized by Eu negative anomaly [61]. After being normalized by chondrite [60], all of the oil shale samples in the Tongchuan and Xunyi areas are well below 0.95, suggesting that the parent rocks of the oil shale come from continental crust. Ce anomalies (δ_{Ce}) of the oil shale samples were close to 1, indicating no obvious abnormality.

The similar North American shale (NASC)-normalized and chondrite-normalized distribution patterns indicate that oil shale samples in the two areas may have formed in an appropriate environment with similar provenance (Figure 5). However, in consideration of the non-negligible difference in concentration of REEs and L/H ratios of oil shale samples of these two areas, the paleo-environment in these two areas is probably the main influence on the discrepancy during oil shale sedimentation. It is noteworthy that heavy rare earth elements show a slightly rich trend, which may be influenced by the absorption of organic matter [62].

4.2 Biomarkers

In this study, sterane distribution of six oil shale samples was examined by *m*/*z* 217 mass chromatograms, and relative amounts of biomarkers were calculated by measuring retention time and peak heights. Peak assignments are listed in Appendix A.

Regular sterane and diasterane are very important for researching maturity and source of organic matter [29, 63−65]. αααC_{29}sterane20S/(20S+20R) and C_{29}streraneββ/(ββ+αα) of oil shale

Table 4 Rare earth elements contents and associated geochemical parameters of oil shale samples from Chang 7 sub-unit (Unit of rare earth elements in ug/g)

Location	Samples No.	La	Ce	Pr	Nd	Sm	Eu	Gd	Tb	Dy	Ho	Er	Tm	Yb	Lu	∑LREE	∑HREE	∑REE	*L*/*H*	δEu	δCe
Xunyi area	ZK2709H1	49.70	100.00	9.55	39.80	7.30	1.52	6.46	1.02	4.89	1.05	3.09	0.52	3.28	0.48	207.90	20.79	228.66	10.00	0.72	1.09
	ZK2709H3	39.30	76.00	7.23	31.00	5.41	1.29	5.52	0.80	4.41	1.06	2.54	0.40	2.52	0.37	160.20	17.62	177.85	9.09	0.77	1.07
	ZK2709H5	39.80	77.80	7.50	30.00	5.46	1.04	5.18	0.90	4.32	0.89	2.66	0.43	2.54	0.37	161.60	17.29	178.89	9.35	0.64	1.07
	ZK2709H6	35.40	66.50	6.59	27.80	5.14	1.19	4.65	0.78	3.56	0.90	2.46	0.34	2.31	0.36	142.60	15.36	157.98	9.29	0.79	1.04
	ZK2709H8	40.90	80.50	7.75	32.90	5.61	1.36	4.93	0.79	3.59	0.85	2.39	0.36	2.26	0.39	169.00	15.56	184.58	10.87	0.84	1.08
	ZK2709H11	43.30	80.50	7.66	33.20	6.16	1.51	5.67	0.84	3.95	0.89	2.35	0.40	2.38	0.35	172.30	16.83	189.16	10.24	0.83	1.05
	ZK2709H12	36.70	75.40	6.97	29.60	5.30	1.15	4.98	0.82	4.06	1.01	2.62	0.42	2.34	0.38	155.10	16.63	171.75	9.33	0.73	1.12
	ZK719H7	46.40	91.50	8.70	35.70	6.29	1.42	5.84	0.85	3.77	0.95	2.51	0.37	2.45	0.42	190.00	17.16	207.17	11.07	0.76	1.08
	ZK719H13	48.00	94.80	9.08	37.80	6.47	1.46	5.54	0.85	3.72	1.01	2.51	0.41	2.44	0.39	197.60	16.87	214.48	11.71	0.79	1.08
	ZK719H16	47.70	94.10	8.96	37.20	6.00	1.47	5.48	0.88	4.09	0.99	2.73	0.45	2.58	0.40	195.40	17.60	213.03	11.10	0.84	1.08
Tongchuan area	ZK1501H3	33.20	62.20	6.43	26.90	5.10	1.13	4.46	0.76	3.28	0.85	1.88	0.36	2.27	0.37	135.00	14.23	149.19	9.48	0.77	1.01
	ZK1501H6	33.10	60.50	6.45	27.30	5.27	1.26	4.76	0.76	3.60	0.95	2.14	0.40	2.70	0.40	133.90	15.71	149.59	8.52	0.82	0.99
	ZK1501H11	29.90	55.80	5.98	26.00	4.77	1.40	4.69	0.72	3.33	0.87	2.02	0.38	2.27	0.38	123.90	14.66	138.51	8.45	0.96	0.99
	ZK1501H13	37.60	68.80	6.88	27.60	4.95	1.38	4.51	0.74	3.16	0.88	1.97	0.37	2.48	0.40	147.20	14.51	161.72	10.15	0.95	1.02
	ZK1501H15	40.40	75.80	8.19	34.90	6.44	1.74	5.74	0.99	4.37	1.21	2.61	0.54	3.19	0.50	167.50	19.15	186.62	8.75	0.93	0.99
	ZK702H6	42.70	82.30	8.81	38.20	7.56	1.14	6.70	1.24	5.91	1.57	3.84	0.76	4.81	0.82	180.70	25.65	206.36	7.05	0.52	1.01
	ZK702H14	34.00	63.50	6.71	28.50	5.07	1.29	4.57	0.74	3.31	0.89	2.04	0.37	2.50	0.37	139.10	14.79	153.86	9.40	0.87	1.00
	ZK702H18	32.70	61.60	6.64	29.20	5.22	1.39	5.11	0.86	3.85	1.01	2.34	0.42	2.73	0.42	136.80	16.74	153.49	8.17	0.88	1.00
	ZK702H24	30.20	55.70	6.06	26.80	5.10	1.52	4.66	0.78	3.66	0.92	2.09	0.40	2.38	0.35	125.40	15.24	140.62	8.23	1.02	0.98
	ZK702H32	35.60	66.90	7.19	30.00	5.33	1.36	4.97	0.78	3.16	0.84	1.97	0.32	2.16	0.36	146.40	14.56	160.94	10.05	0.86	1.00
Xunyi area(average)		42.70	83.70	8.00	33.50	5.90	1.30	5.40	0.90	4.00	1.00	2.60	0.40	2.50	0.40	175.18	17.17	192.35	10.21	0.77	1.08
Tongchuan area(average)		34.94	65.31	6.93	29.54	5.48	1.36	5.02	0.84	3.76	1.00	2.29	0.43	2.75	0.44	143.57	16.52	160.09	8.82	0.86	1.01
NASC[b]		32.00	73.00	7.90	33.00	5.70	1.24	5.20	0.85	5.80	1.04	3.40	0.50	3.10	0.48	152.84	20.37	173.21	7.50	—	—
Chondrite[c]		0.31	0.81	0.12	0.60	0.20	0.07	0.26	0.05	0.32	0.07	0.21	0.03	0.21	0.03	2.11	1.18	3.29	4.47	—	—

[b] Cited from HASKIN et al [59]. [c] Cited from TAYLOR and MCLENNAN [60]. Note: ∑LREE: total content of light rare earth elements (∑LREE=La+Ce+Pr+Nd+Sm+Eu); ∑HREE: total content of heavy rare earth elements (∑HREE=Gd+Tb+Dy+Ho+Er+Tm+Yb+Lu); ∑REE: total content of rare earth elements (∑REE=∑LREE+∑HREE); *L*/*H*=∑LREE/∑HREE; $\delta_{Eu}=Eu_n/(Sm_n\times Gd_n)^{1/2}$; $\delta Ce=Ce_n/(La_n\times Pr_n)^{1/2}$; n: Chondrite-normalized.

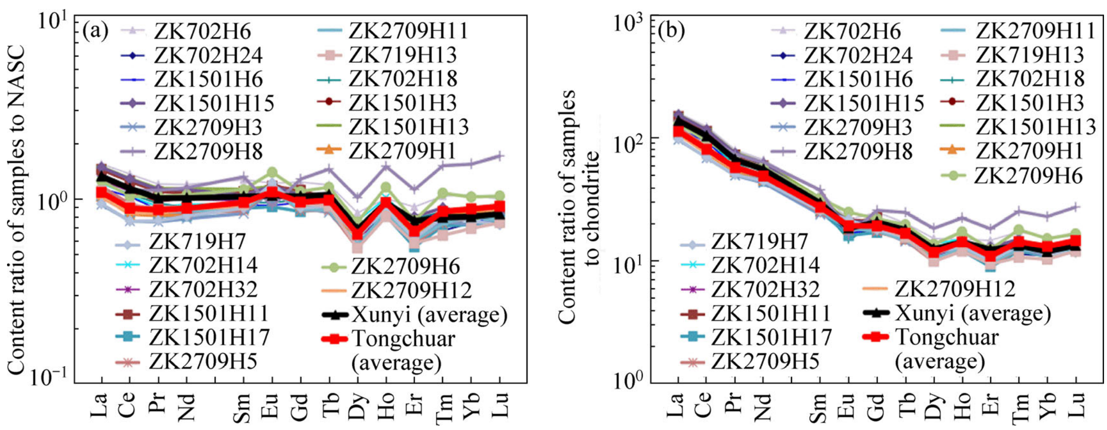

Figure 5 NASC-normalized REEs distribution pattern of oil shale samples (a) and chondrite-normalized REEs distribution pattern of oil shale samples (b). These two distribution patterns show that oil shale in these two areas formed in an appropriate environment with similar provenance

samples in the southern Ordos Basin vary over a small range (Tongchuan area: 0.49−0.5 and 0.36−0.43; Xunyi area: 0.45−0.46 and 0.36−0.39, respectively), demonstrating that the oil shale in these two areas has reached similar maturity. The total concentration of regular steranes is primarily composed of C_{29}(41.6%−49.0%, averaging 43.6%), with relatively low contents of C_{27}(25.0%−36.1%, averaging 30.3%) and C_{28}(19.8%−33.0%, averaging 26.1%) in all oil shale samples. The distribution and content of sterane in oil shale samples in the Tongchuan area and Xunyi area are very similar (Figure 6), indicating that the oil shale in the southern Ordos Basin has a homologous organic matter source.

5 Discussion

5.1 Sources and maturity level of organic matter

Based on several analysis methods (rock pyrolysis, element C, H and O analysis, carbon isotope and saturated hydrocarbon mass chromatogram), the organic matter source of the oil shale from the Chang 7 sub-unit in the southern Ordos Basin is considered to be primarily algae [66−70]. However, the oil shale samples were

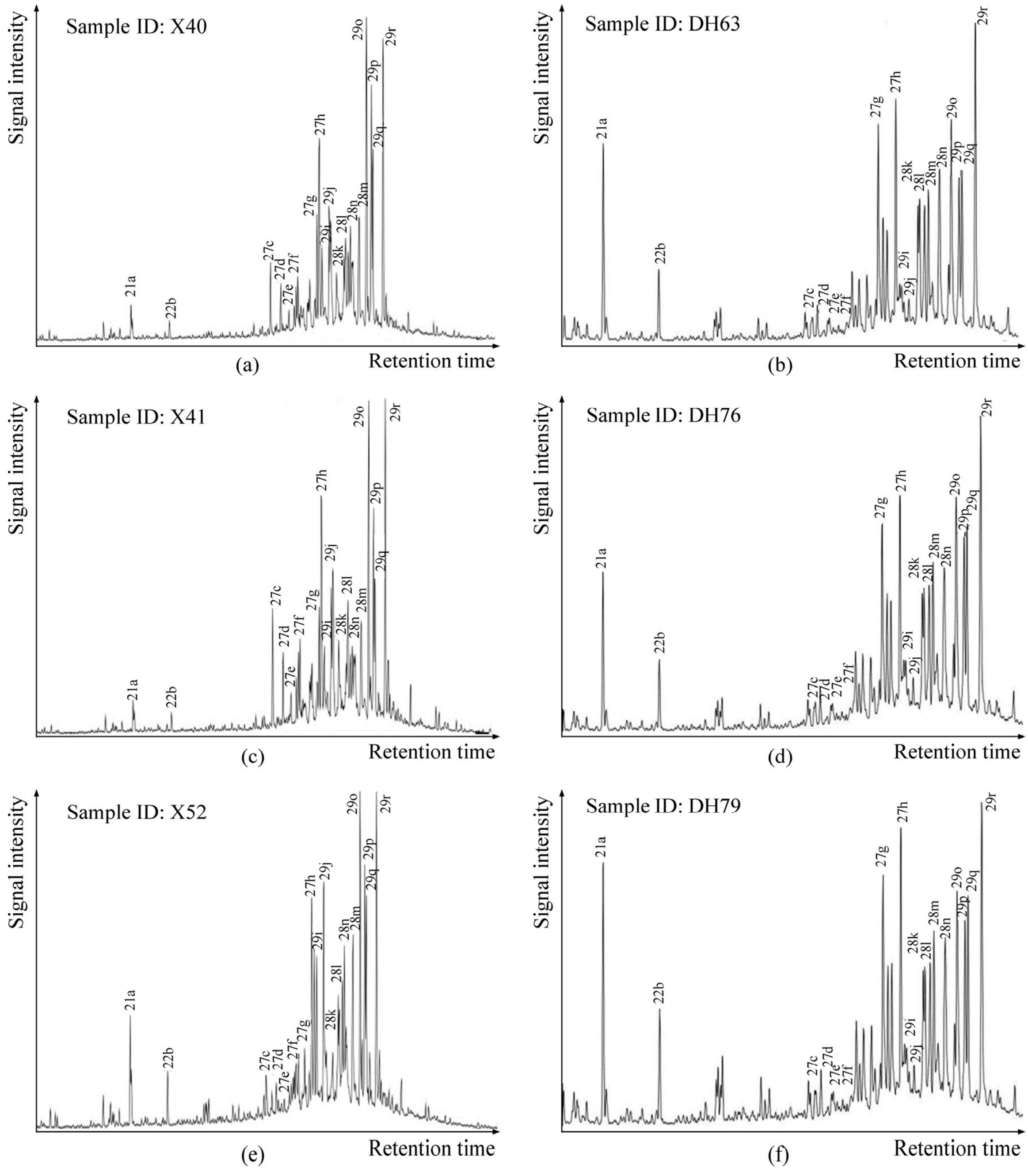

Figure 6 *m*/*z* 217 mass fragmentograms of saturated hydrocarbon fractions of six representative oil shale samples in Tongchuan and Xunyi areas. The left and right three oil shale samples were collected from Xunyi area and Tongchuan area, respectively, demonstrating the organic matter sources of oil shale

primarily collected in outcrops, and weathering and biodegradation can have a substantial influence on the above analysis methods. In particular, when oil shale samples reach maturity, a saturated hydrocarbon mass chromatogram can wrongly reflect the source of organic matter. In a mass chromatogram of steranes, C_{27}, C_{28} and C_{29} regular steranes are negligibly affected by weathering and biodegradation, and can provide a good explanation of the source of organic matter [29, 30, 63]. Generally, C_{27} and C_{28} regular steranes are primarily from lower aquatic organisms (e.g., various algae), and the C_{29} regular sterane is typically from advanced plants [29]. By analyzing the relative content of regular steranes, the source of organic matter in oil shale was determined to be of mixed type, indicating that the source of organic matter in oil shale from the Chang 7 sub-unit in the southern Ordos Basin is a blend of lower aquatic organisms and advanced plants (Figure 7(a)), rather than merely algae.

In addition, the maturity of the Chang 7 source rock in the southern Ordos Basin remains controversial. Based on the analysis of vitrinite reflectance (*R*o), different scholars hold different opinions concerning maturity. The differences related to the use of different laboratory instruments, as well as unsystematic samples. Biomarker ratios are less affected by experimental error and can provide an accurate indication for maturity. The regular steroids 14 and 17(H) are converted from the αα configuration to the ββ configuration during the evolution of steroid series [30, 71−72]. αααC_{29}sterane20S/(20S+20R) and C_{29}streraneββ/(ββ+αα) are usually used to investigate maturity, and increase with increasing degrees of maturity [3, 73]. As discussed in section 4.2, αααC_{29}sterane20S/(20S+20R) and C_{29}streraneββ/(ββ+αα) ratios of the oil shale samples show that the oil shale in the southern Ordos Basin has reached maturity (Figure 7(b)).

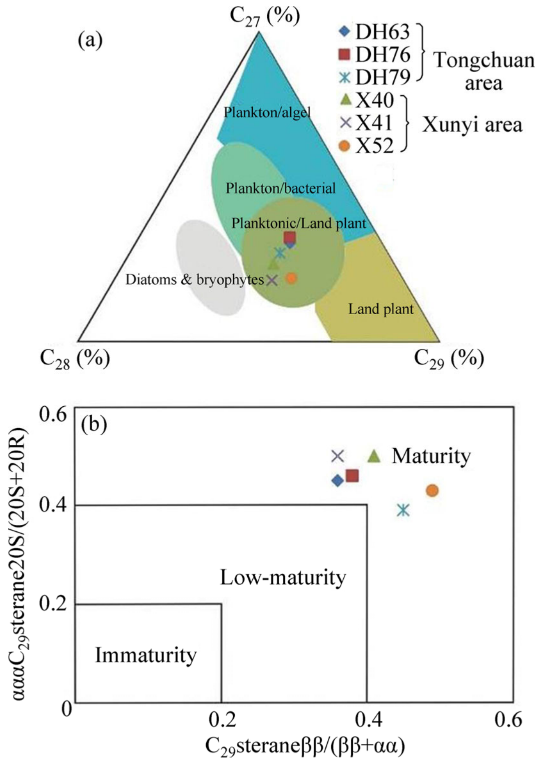

Figure 7 Ternary diagram of C_{27}, C_{28} and C_{29} terane compositions of oil shale samples, showing that source of organic matter of oil shale samples in southern Ordos Basin is mixed matter, comprising lower aquatic organisms and advanced plants. The base map is from YANDOKA et al [31] (a) and cross plot (b) of αααC_{29}sterane20S/(20S+20R) versus C_{29}streraneββ/(ββ+αα) of oil shale samples, reflecting that oil shale in southern Ordos Basin has reached maturity. The base map is from LI et al [30] and DUAN et al [64] (b)

5.2 Paleoenvironment comparison

Although the Tongchuan and Xunyi areas are all in semi-deep to deep lake facies, the paleo-environment in these two areas must have been different due to the tectonic setting, leading to a distinct redox condition, paleoclimate, sedimentation rate, etc [37]. Several single elements can provide good representation of the environment, including U, Ni and V [74−79]. However, due to limitations in the application and contingency of sampling, these elements cannot accurately describe the environment variation. Element ratios are sensitive to the paleo-environment, and achieve a good effect in a lacustrine environment [75, 78]. Therefore, in the current study, several element ratios are considered in the discussion of the different environments of the two areas.

U, Ni and V are sensitive to the redox condition. Thus, U/Th is generally applied to reconstructing the redox condition; gradual increases in the ratio are associated with the redox condition turning anoxic [3, 39, 78]. Similarly, V/Ni can also reflect the redox condition; a ratio over 1 indicates an anoxic condition, whereas a ratio below 1 reflects an oxic condition [15, 78]. The

V/Ni ratios of the oil shale samples were all over 1, indicating the presence of anoxic conditions during oil shale sedimentation in the southern Ordos Basin. Further, the U/Th and V/Ni ratios of oil shale samples in the Tongchuan area (averaging 3.92; 8.76) were clearly larger than those in the Xunyi area (averaging 0.73; 4.23), indicating that the degree of anoxic condition in the Tongchuan area is higher and more beneficial for organic matter preservation (Figures 8(a) and (b)).

The geochemical behavior of Sr and Ba is very similar [18, 39, 56]. However, when the mineralization of water increases together with increase in salinity, Ba deposits in the form of $BaSO_4$ first. Sr deposits when salinity concentrates to a certain extent [18, 39, 56]. Thus, Sr/Ba can be used to reflect salinity. Generally, Sr/Ba >1, 0.6−1, and <0.6 reflect sea water, brackish water, and fresh water, respectively [3, 78]. The Sr/Ba of oil shale samples in the study area ranged from 0.23 to 0.69, except for one sample that was over 0.6 (ZK1501H13), suggesting that the oil shale primarily deposited in fresh water. The Sr/Ba ratios of oil shale samples in the Tongchuan area (0.29−0.69, averaging 0.45) were higher than those in the Xunyi area (0.23−0.39, averaging 0.31), indicating that the paleosalinity in the Tongchuan area is slightly higher than that of the Xunyi area (Figure 8(c)). Previous studies have shown that relatively high paleosalinity is good for the preservation of organic matter [18, 76, 79]. Thus, in view of the preservation condition, the Tongchuan area is better than the Xunyi area.

Several pieces evidence, such as micro-and nannofossils [80], tuff (Figure 9(a)) [38, 39], high gamma sandstone [81], syndepositional structure (Figure 9(b)), have indicated the existence of hydrothermal fluid activities during oil shale sedimentation in the southern Ordos Basin. However, there is a lack of evidence evaluating the intensity of the hydrothermal fluid activities. Element ratios, particularly Fe/Ti, can provide evidence of hydrothermal fluid activities, as well as intensity. When Fe/Ti is over 20, it is indicated that the sediments are affected by obvious hydrothermal fluid activities, and the intensity becomes stronger with the increase in the Fe/Ti ratio [82]. The Fe/Ti ratios of the oil shale samples in the Xunyi area are all below 20 (8.68−18.37, averaging 12.96), and the ratios in the Tongchuan area are mostly over 20(15.22−37.57, averaging 28.45), with one exception (ZK1501H13). These findings provide evidence of obvious hydrothermal fluid activities in the Tongchuan area (Figure 8(d)). The hydrothermal fluid activities can bring about some saline material, which could be the main reason for the paleosalinity discrepancy between the two areas. In lacustrine sediments, hydrothermal fluid can have a positive effect, not only on the organic matter enrichment, but also on its preservation [11, 83]. Thus, oil shale in the Tongchuan area has higher organic matter abundance and more superior preservation conditions than the Xunyi area.

The Sr/Cu ratio of sediments is sensitive to climate and can be used to reconstruct the paleoclimate [18, 56]. Ratios of 1−10 and >10 indicate a warm and humid climate, and a dry and hot climate, respectively. The average value of the Xunyi and Tongchuan areas was 0.31 and 0.45, respectively, with all samples within a narrow range. This indicates that the paleoclimate in these two areas is warm and humid (Figure 8(e)).

La and Yb are differentiated by electrovalence and adsorbing ability as the environment changes [24,84]. When the detention time is short, sediments deposit sharply and the $(La/Yb)_{NASC}$ approaches to 1. On the other hand, long detention time leads to adequate physicochemical reactions and the $(La/Yb)_{NASC}$ deviates from 1. Figure 8(f) shows that the $(La/Yb)_{NASC}$ values of samples from the Xunyi area are fundamentally higher than those from the Tongchuan area, suggesting that the sedimentary rate of the Tongchuan area is lower than that of the Xunyi area and the paleo-water-depth in the Tongchuan area is deeper than that in the Xunyi area. The low sedimentary rate is beneficial for the preservation of organic matter.

Fe and Co are congener elements with similar physicochemical properties. In a nearshore lacustrine environment, Fe deposits more than Co, and the Co concentration increases with increasing water depth [85]. Therefore, the Fe/Co ratio can indicate the relative water depth, and increases with decreasing values of the ratio. The Fe/Co ratios of the oil shale samples in the Tongchuan area (2645.76−11421.05, averaging 5868.92) are mostly lower than those in the Xunyi area (6426.23−17919.29, averaging 9283.30), indicating that the paleo-water-depth in the Tongchuan area is deeper than that in the Xunyi area (Figure 8(g)). In addition, Th/U can also be applied to judging water depth; higher ratios indicate deeper water [85, 86].

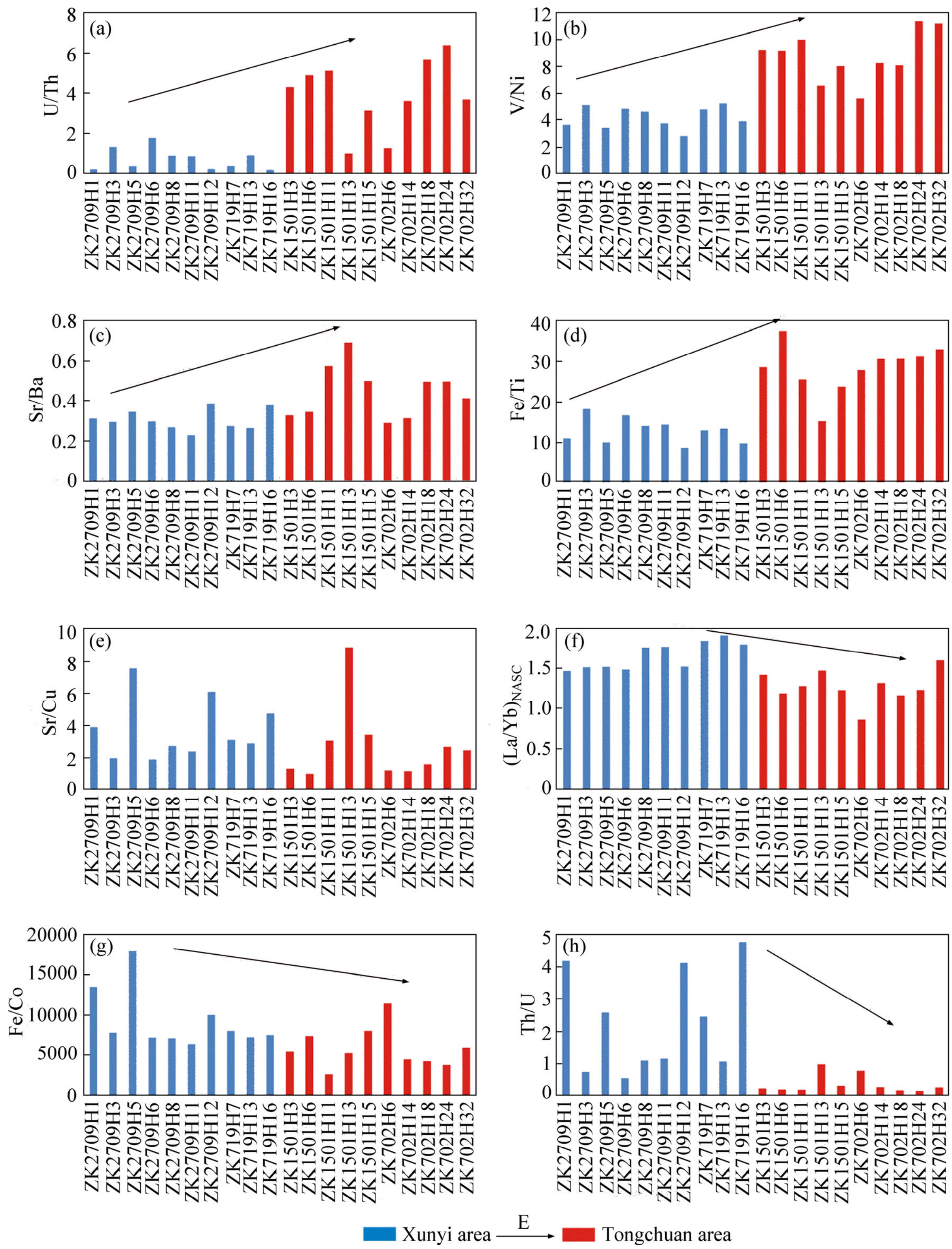

Figure 8 Comparison of elements geochemistry parameters and paleoenvironment of oil shale samples in Tongchuan and Xunyi areas. The comparison of redox proxies (U/Th and V/Ni) indicates that redox condition during the Chang 7 oil shale sedimentation in Tongchuan area is more reducing than that of Xunyi area. The paleosalinity proxy (Sr/Ba) comparisons show that salinity of Tongchuan area is higher than that of Xunyi area, benefiting oil shale preservation. The hydrothermal fluid activities proxy (Fe/Ti) comparison illustrated that the Tongchuan area experienced stronger hydrothermal fluid effects than the Xunyi area. The paleoclimate proxy (Sr/Cu) comparison between the two areas showed no discrepancy. The sedimentary rate proxy ($(La/Yb)_{NASC}$) comparison indicated that the oil shale in the Tongchuan area deposit is more stable than that of the Xunyi area. Comparison of the paleo-water-depth proxies (Fe/Co and Th/U) demonstrated that the depth of the water in the Tongchuan area is deeper than that of the Xunyi area

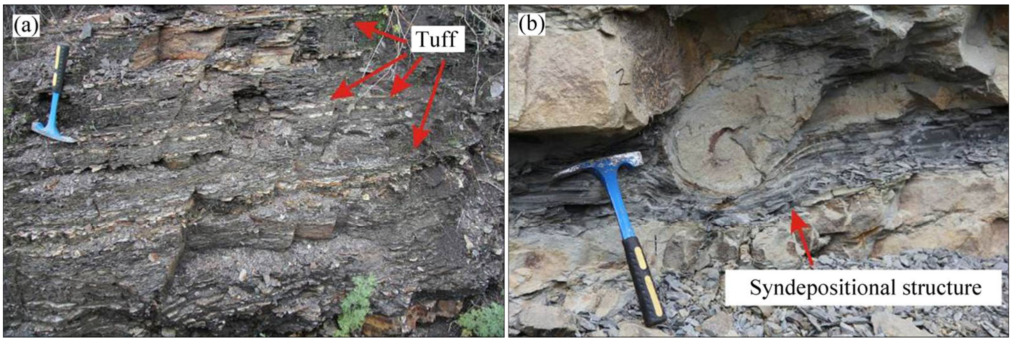

Figure 9 Tuff (a) and syndepositional structure (b) of oil shale section in Yishicun profile, Tongchuan area, indicating obvious hydrothermal fluid activities in southern Ordos Basin

Oil shale samples from the Tongchuan area (0.16−0.98, averaging 0.36) show lower Th/U ratios than those in the Xunyi area (0.56−4.76, averaging 2.27) (Figure 8(h)), similar to the findings for the Fe/Co ratio. The deeper the water is, the more space there is for organic matter to deposit in. Therefore, the Tongchuan area is better for the formation and preservation of oil shale.

5.3 Depositional model

Previous studies have indicated that the paleo-productivity of the lake in the southern Ordos Basin is relatively high, with an average (TOC) in the oil shale of 16.04 wt% [14]. According to oil yield statistics, the average oil yield of the oil shale from the Tongchuan area (>5.5 wt%) is significantly higher than that from the Xunyi area (4.5 wt%−5.5 wt%) [15, 18, 56]. The oil yield of oil shale is positively correlated with TOC; the relationship can be expressed as T=2.79×w+0.907, where T and w represent the TOC (wt%) and oil yield (wt%), respectively [18]. After calculating the TOC, the results indicate that the average TOC of the oil shale from the Tongchuan area is above 16.25 wt%, whereas the corresponding value from the Xunyi area is below this; this may be a result of the sedimentary environment differences between the areas. During oil shale sedimentation, tectonic and volcanic orogenies in the southern Ordos Basin play an important role in the formation of oil shale. The liquefied sandstone vein that can be seen in sections of the oil shale further supports this (Figure 10(a)). With regard to plate movement, the Triassic Indosinian movement causes the Qinling paleooceanic to subduct to the North China Plate, forming an active continental margin with the trench-arc-basin system [87]. The southern Ordos Basin then gradually subsides. During the Chang 7 period, the depression reaches its maximum, receiving a large amount of organic matter and terrestrial detrital material, which primarily comes from the south. The siltstone granularity analysis of the oil shale interlayer indicates that part of the clastic rocks entering into the lake are in the form of turbidite [88], and higher terrestrial plant fossils can be seen in the sandstone interlayers (Figure 10(b)). This suggests that higher terrestrial plants are accompanied by tectonic orogenies, entering into the lake. Thus, organic matter input of the oil shale is dominated by algae and terrestrial plants, contributing to the material base of the oil shale. The hydrothermal fluid activity caused by volcanic eruption plays an important role in the enrichment of the organic matter in the oil shale. HE et al [83] and HE et al [11] suggested that hydrothermal fluid activities can not only supply nutrient elements, but can also enhance the reducibility of the lake, which is beneficial to oil shale preservation. Further, thermal fluid accelerates the death of organisms, which also has a positive effect on the enrichment of organic matter in oil shale [65−70]. The strong reducing condition of the water body is also conducive to the preservation of the organic matter. The relatively deep water provides not only low oxygen, but also weak hydrodynamic force, and the stable sedimentary condition is good for biodegradation. The warm and humid climate is beneficial to the biological development, providing a favorable physical basis for the oil shale. Influenced by the reducing condition, thermal fluid activities, slow deposition rate, warm and humid paleoclimate, and fresh water, the oil shale from the Chang 7 sub-unit in the southern Ordos Basin is well developed (Figure 11). In view of the paleoenvironment, the oil shale in the Tongchuan area is superior to that in

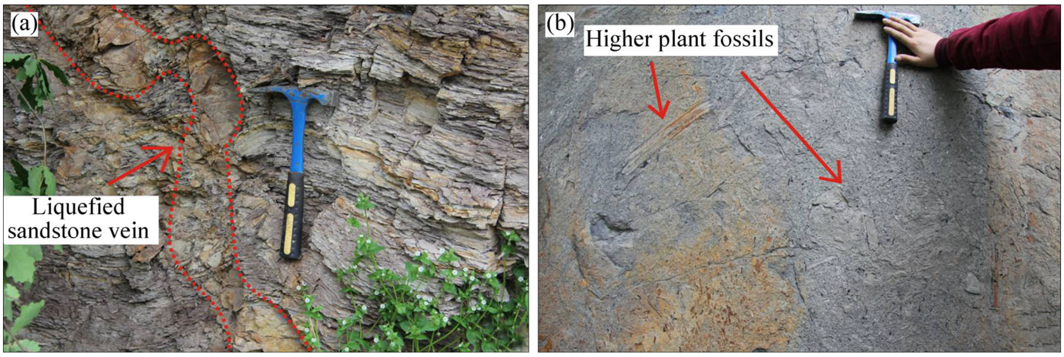

Figure 10 Liquefied sandstone vein (a) and higher plant fossils (b) across the oil shale section in Yishicun profile, Tongchuan area. Liquefied sandstone vein results from an earthquake event, suggesting intense tectonic and volcanic orogenies. Higher plant fossils occur with turbidite, implying that event deposits are the main pattern for higher plants entering the lake

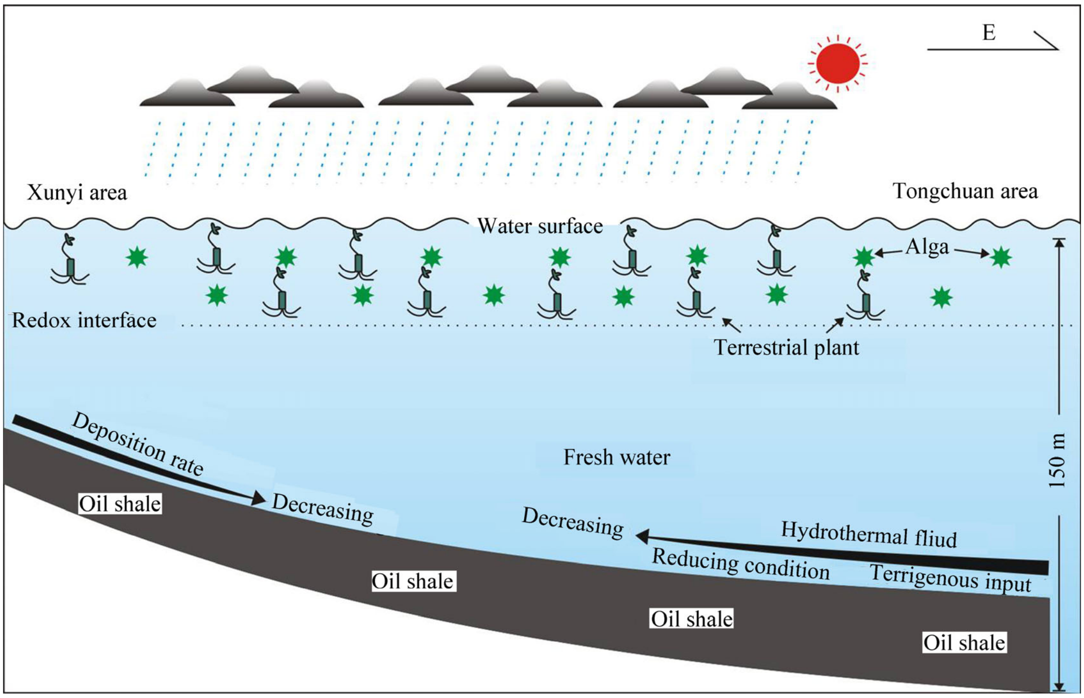

Figure 11 Depositional model of Chang 7 oil shale of Triassic Yanchang Formation in Tongchuan and Xunyi areas in southern Ordos Basin. The oil shale deposited in warm and humid weather with a relatively light water body. From the Tongchuan area to Xunyi area, hydrothermal fluid activities, and reducing condition and terrigenous input gradually decrease with increasing deposition rate. The organic matter sources of oil shale are dominated by algae and terrestrial plants, with a superior preservation environment facilitating the formation of the oil shale

Table 5 Biomarker parameters of *m*/*z* 217 of oil shale samples

Location	Samples No.	αααC_{29}sterane20S/(20S+20R)	C_{29}streraneββ/(ββ+αα)	Regular sterane/%		
				C_{27}	C_{28}	C_{29}
Tongchuan area	DH63	0.45	0.36	26.0	31.0	43.0
	DH76	0.46	0.38	25.0	33.0	42.0
	DH79	0.45	0.39	29.9	28.5	41.6
Xunyi area	X40	0.50	0.41	31.2	19.8	49.0
	X41	0.50	0.36	36.1	20.1	43.8
	X52	0.49	0.43	33.6	24.3	42.1

Table 6 Elements geochemistry parameters of paleoenvironment of oil shale samples in Tongchuan and Xunyi areas

Location	Samples No.	U/Th	V/Ni	Sr/Ba	Fe/Ti	Sr/Cu	$(La/Yb)_{NASC}$	Fe/Co	Th/U
Xunyi area	ZK2709H1	0.24	3.65	0.31	11.03	3.91	1.47	13471.70	4.18
	ZK2709H3	1.35	5.15	0.30	18.37	1.97	1.51	7825.84	0.74
	ZK2709H5	0.39	3.44	0.35	10.03	7.57	1.52	17919.29	2.59
	ZK2709H6	1.80	4.85	0.30	16.74	1.90	1.48	7240.00	0.56
	ZK2709H8	0.91	4.63	0.27	14.09	2.77	1.75	7122.81	1.10
	ZK2709H11	0.86	3.76	0.23	14.42	2.39	1.76	6426.23	1.16
	ZK2709H12	0.24	2.83	0.39	8.68	6.12	1.52	10012.66	4.12
	ZK719H7	0.41	4.79	0.27	13.05	3.14	1.83	8040.54	2.46
	ZK719H13	0.93	5.26	0.27	13.42	2.92	1.91	7270.97	1.07
	ZK719H16	0.21	3.91	0.38	9.81	4.77	1.79	7502.99	4.76
Tongchuan area	ZK1501H3	4.32	9.22	0.33	28.63	1.33	1.42	5449.37	0.23
	ZK1501H6	4.90	9.19	0.35	37.57	1.01	1.19	7407.41	0.20
	ZK1501H11	5.13	9.99	0.57	25.59	3.09	1.28	2645.76	0.19
	ZK1501H13	1.02	6.60	0.69	15.22	8.84	1.47	5261.67	0.98
	ZK1501H15	3.13	8.04	0.50	23.84	3.45	1.23	8045.98	0.32
	ZK702H6	1.28	5.63	0.29	27.96	1.22	0.86	11421.05	0.78
	ZK702H14	3.63	8.27	0.31	30.68	1.16	1.32	4472.22	0.28
	ZK702H18	5.68	8.09	0.50	30.72	1.59	1.16	4264.90	0.18
	ZK702H24	6.39	11.37	0.50	31.29	2.71	1.23	3768.49	0.16
	ZK702H32	3.70	11.19	0.41	33.01	2.48	1.60	5952.38	0.27
Xunyi area(average)		0.73	4.23	0.31	12.96	3.75	1.65	9283.30	2.27
Tongchuan area(average)		3.92	8.76	0.45	28.45	2.69	1.27	5868.92	0.36

the Xunyi area, suggesting that the Tongchuan area is the key exploration area in the southern Ordos Basin.

6 Conclusions

This paper compares the depositional conditions of oil shale from the Tongchuan and Xunyi areas of the Chang 7 sub-unit, and summarizes a depositional model of the oil shale from the southern Ordos Basin. Several conclusions are outlined below:

1) Element geochemistry characteristics indicate that the Al_2O_3/TiO_2 ratios of oil shale samples range between 21.67 and 46.69, illustrating that the parent rock of oil shale in the southern Ordos Basin is felsic igneous rocks. Si/(Si+Al+Fe) ratios of the oil shale samples suggest that the sediment location of the oil shale is not far from the terrigenous provenance. U and Cu are enriched in the oil shale samples, indicating that the content of organic matter in the oil shale is high. The concentration and distribution pattern of rare earth elements indicates that the oil shale in the southern Ordos Basin is deposited in a similar paleoenvironment. However, the characteristics of the major elements, trace elements, and rare earth elements in oil shale samples from the Tongchuan and Xunyi areas are significantly different, which may reflect the depositional conditions.

2) The sterane distribution of six oil shale samples is very similar, and the C_{29} concentration is higher than the C_{27} and C_{28} concentrations, suggesting that the oil shale in the southern Ordos Basin has a homologous organic matter source, with the organic matter being of mixed origin comprising lower aquatic organisms and advanced plants. αααC_{29}sterane20S/(20S+20R) and C_{29}streraneββ/(ββ+αα) ratios of the oil shale samples vary only slightly (Tongchuan area: 0.49−0.5 and 0.36−0.43; Xunyi area: 0.45−0.46 and 0.36−0.39, respectively), and indicate that the oil shale has reached maturity.

3) U/Th and V/Ni ratios suggest that the redox

condition is dominated by a reducing condition, and the anoxic degree of the Tongchuan area is higher than that of the Xunyi area. Sr/Ba ratios illustrate that the oil shale is deposited in fresh water and the paleosalinity in the Tongchuan area is slightly higher than that in the Xunyi area. Fe/Ti ratios imply that the Tongchuan area has gone through obvious hydrothermal fluid activities, while the Xunyi area has not. Sr/Cu ratios indicate a warm and humid paleoclimate in both areas, with no obvious difference between the two areas. The $(La/Yb)_{NASC}$ indicates that the deposition rate in the Tongchuan area is lower than that in the Xunyi area. Fe/Co and Th/U ratios indicate that the paleo-water-depth in the Tongchuan area is deeper than that in the Xunyi area.

4) In light of the paleoenvironment of oil shale in the southern Ordos Basin, a depositional model of the oil shale is proposed. Compared with the Xunyi area, the Tongchuan area appears to be the key exploration area for the oil shale in the Chang 7 sub-unit of the southern Ordos Basin.

Appendix A:

Peak assignments for *m*/*z* 217 mass fragmentograms of saturated hydrocarbon fractions

Peak No.	Compound name
21a	5α(H),14β(H)-pregnane
22b	5α(H),14β(H)-homopregnane
27c	13β(H),17α(H)-diacholestanes 20S
27d	13β(H),17α(H) - diacholestanes 20R
27e	5α(H),14α(H),17α(H) – cholestanes 20S
27f	5α(H),14β(H),17β(H) – cholestanes 20R
27g	5α(H),14β(H),17β(H) - cholestanes 20S
27h	5α(H),14α(H),17α(H) – cholestanes 20R
29i	24-ethyl-13β(H),17α(H)-diacholestanes 20R
29j	24-ethyl-13β(H),17α(H)-diacholestanes 20S
28k	24-methyl-5α(H),14α(H),17α(H)-cholestanes 20S
28l	24-methyl-5α(H),14β(H),17β(H)-cholestanes 20R
28m	24-methyl-5α(H),14β(H),17β(H)-cholestanes 20S
28n	24-methyl-5α(H),14α(H),17α(H)-cholestanes 20R
29o	24-ethyl-5α(H),14α(H),17α(H)-cholestanes 20S
29p	24-ethyl-5α(H),14β(H),17β(H)-cholestanes 20R
29q	24-ethyl-5α(H),14β(H),17β(H)-cholestanes 20S
29r	24-ethyl-5α(H),14α(H),17α(H)-cholestanes 20R

References

[1] LIU R, LIU Z, GUO W, CHEN H. Characteristics and comprehensive utilization potential of oil shale of the Yin'e basin, inner Mongolia, China [J]. Oil Shale, 2015, 32(4): 293−312.

[2] LIU Zhao-jun. Oil shale in China [M]. Beijing: Petroleum Industry Press, 2009. (in Chinese)

[3] LI D, LI R, ZHU Z, WU X, CHENG J, LIU F, ZHAO B. Origin of organic matter and paleo-sedimentary environment reconstruction of the Triassic oil shale in Tongchuan City, southern Ordos Basin (China) [J]. Fuel, 2017, 208: 223−235.

[4] HAKIMI M H, WAN H A, ALQUDAH M, MAKEEN Y M, MUSTAPHA K A. Organic geochemical and petrographic characteristics of the oil shales in the Lajjun area, Central Jordan: Origin of organic matter input and preservation conditions [J]. Fuel, 2016, 181: 34−45.

[5] SONG Y, LIU Z, MENG Q, XU J, SUN P, CHENG L, ZHENG G. Multiple controlling factors of the enrichment of organic matter in the upper cretaceous oil shale sequences of the Songliao Basin, NE China: Implications from geochemical analyses [J]. Oil Shale, 2016, 33(2): 142−166.

[6] LV D W, LI Z X, LIU H Y, LI Y, FENG T T, WANG D D, WANG P L, LI S Y. The characteristics of coal and oil shale in the coastal sea areas of Huangxian Coalfield, Eastern China [J]. Oil Shale, 2015, 32(3): 204−207.

[7] ŞENGÜLER İ, KARA-GÜLBAY R, KORKMAZ S. Organic geochemical characteristics of miocene oil shale deposits in the Eskişehir Basin, western Anatolia, Turkey [J]. Oil Shale 2014, 31(4): 315−336.

[8] MORADI A V, SARI A. Evaluation of the hydrocarbon potential, mineral matrix effect and gas-oil ratio potential of oil shale from the Kabalar Formation, Göynük, Turkey [J]. Oil Shale, 2015, 32(1): 25−42.

[9] LIU B, BECHTEL A, SACHSENHOFER R F, GROSS D, GRATZER R, CHEN X. Depositional environment of oil shale within the second member of permian lucaogou formation in the santanghu basin, northwest China [J]. International Journal of Coal Geology, 2017, 175: 10−25. DOI: 10.1016/j.coal.2017.03.011.

[10] KALLEMETS K. Economic sustainability of estonian shale oil industry until 2030 [J]. Oil Shale, 2016, 33(3): 272−289.

[11] HE Cong, JI Li-ming, SU Ao, LIU Ying, LI Jian-feng, WU Yuan-dong, ZHANG Ming-zhen. Relationship between hydrothermal sedimentation process and source rock development in the Yanchang Formation, southern Ordos Basin [J]. Earth Science Frontiers, 2017, 24(6): 277−285. (in Chinese)

[12] JIA J, LIU Z, MENG Q, LIU R, SUN P, CHEN Y. Quantitative evaluation of oil shale based on well log and 3-D seismic technique in the Songliao Basin, Northeast China [J]. Oil Shale, 2012, 29(2): 128−150.

[13] BAI Yun-lai, MA Long, WU Wu-jun, MA Yu-hu. Geological characteristics and resource potential of oil shale in Ordos basin [J]. Geology in China, 2009, 36(5): 1123−1137. (in Chinese)

[14] ZHANG Qing-chun, WANG Kai-ming, LUO Shun-she, WU

Xiao-zhi. Study on the characteristics and origin of the oil shale in the Chang 7 Member, Yanchang formation in Ordos Basin [J]. Advances in Geosciences, 2013, 3(4): 197−209. (in Chinese)

[15] MA Zhong-hao, CHEN Qing-shi, SHI Zhong-wang, WANG Cheng, DU Wu-gang, ZHAO Chang-ying. Geochemistry of oil shale from Chang 7 reservoir of Yanchang Formation in south Ordos Basin and its geological significance [J]. Geological Bulletin of China, 2016, 35(9): 1550−1558. (in Chinese)

[16] LUO Yin-shan, ZHANG Shao-nan, ZHANG Zhi-huan, DENG Nan-tao, HE Yong-hong, LIANG Quan-sheng. Favorable area forecast of oil shale exploration in southern Ordos basin [J]. China Mining Magazine, 2014, 23(1): 83−86. (in Chinese)

[17] ZHANG Cai-li, GAO A-long, LIU Zhe, HUANG Jing, YANG Ya-juan, ZHANG Yan. Study of character on sedimentary water and palaeoclimate for Chang7 oil layer in Ordos Basin [J]. Natural Gas Geoscience, 2010(4): 582−587. (in Chinese)

[18] SUN Sha-sha, LIU Ren-he, BAI Wen-hua. Effect factor analysis of oil content of upper triassic oil shale in Tongchuan area, Ordos Basin [J]. China Petroleum Exploration, 2011, 6(2): 79−83. (in Chinese)

[19] DENG Nan-tao, ZHANG Zhi-huan, REN Lai-yi, WANG Fu-bin, LIANG Quan-sheng, LI Yu-xiang, LI Wen-hao, ZHAO Shuang-feng, LUO Meng-jiao. Geochemical characteristics and distribution rules of oil shale from Yanchang Formation, Southern Ordos Basin [J]. Petroleum Geology and Experiment, 2013, 35(4): 432−437. (in Chinese)

[20] FU Xiu-gen, WANG Jiang, ZENG Yu-hoong, TAN Fu-wen, FENG Xing-lei. REE geochemistry of marine oil shale from the Changshe Mountain area, northern Tibet, China [J]. International Journal of Coal Geology, 2010, 81(3): 191−199.

[21] FU Xiu-gen, WANG Jian, CHEN Wen-bin, FENG Xing-lei, WANG Dong, SONG Chun-yan, ZENG Sheng-qiang. Elemental geochemistry of the early Jurassic black shales in the Qiangtang Basin, eastern Tethys: Constraints for palaeoenvironment conditions [J]. Geological Journal, 2016, 51(3): 443−454.

[22] LI De-lu, LI Rong-xi, ZHU Zeng-wu, XU Feng. Elemental characteristics of lacustrine oil shale and its controlling factors of palaeo-sedimentary environment on oil yield: A case from Chang 7 oil layer of Triassic Yanchang Formation in southern Ordos Basin [J]. Acta Geochimica, 2018(2): 1−16.

[23] WANG Zhong-wei, FU Xiu-gen, FENG Xing-lei, SONG Chun-yan, WANG Dong, CHEN Wen-bin, ZENG Sheng-qiang. Geochemical features of the black shales from the Wuyu Basin, southern Tibet: Implications for palaeoenvironment and palaeoclimate [J]. Geological Journal, 2015, 52: 282−297.

[24] LI De-lu, LI Rong-xi, ZHU Zeng-wu, WU Xiao-li, ZHAO Bang-sheng, CHEN Jing-hua, LIU Fu-tian. Rare earth elements geochemistry characteristics and their geological implications of lacustrine oil shale from Chang 7 oil layer in southern Ordos Basin, China [J]. Geological Journal, 2017, 52(S1). DOI: 10.1002/gj.2980.

[25] FU Xiu-gen, WANG Jian, ZENG Yu-hong, TAN Fu-wen, FENG Xing-lei, CHEN Wen-bin. The geochemistry of platinum group elements in marine oil shale—A case study from the Bilong Co oil shale, northern Tibet, China [J]. Chemie der Erde–Geochemistry, 2015, 75(2): 55−63.

[26] LI De-lu, LI Rong-xi, WU Xiao-li, LIU Fu-tian, ZHAO Bang-sheng, WANG Bao-ping. Influence on lacustrine source rock by hydrothermal fluid: A case study of the Chang 7 oil shale, southern Ordos Basin [J]. Acta Geochimica, 2018(2): 1−13. DOI: 10.1007/s11631-017- 0203-1.

[27] ZENG Sheng-qiang, WANG jian, FU Xiu-gen, CHEN Wen-bin, FENG Xiang-lei, WANG Dong, SONG CHUN-yan, WANG Zhong-wei. Geochemical characteristics, redox conditions, and organic matter accumulation of marine oil shale from the Changliang Mountain area, northern Tibet, China [J]. Marine & Petroleum Geology, 2015, 64: 203−221.

[28] YUAN W, LIU G, STEBBINS A, XU L, NIU X, LUO W, LI C. Reconstruction of redox conditions during deposition of organic-rich shales of the Upper Triassic Yangchang Formation, Ordos Basin, China [J]. Palaeogeography Palaeoclimatology Palaeoecology, 2016, 486: 158−170, DOI: 10.1016/j.palaeo.2016.12.020.

[29] ZHAO Yang, YAO Jing-li, DUAN Yi, WU Ying-zhong, CAO Xi-xi, Xu Li, CHEN Shan-shan. Oil-source Analysis for Chang-9 Subsection (Upper Triassic) of Eastern Gansu Province in Ordos Basin [J]. Acta Sedimentologica Sinica, 2015, 33: 1023−1032. (in Chinese)

[30] LI De-lu, LI Rong-xi, WANG Bao-ping, LIU Zhi, WU Xiao-li, LIU Fu-tian, ZHAO Bang-sheng. Study on oil-source correlation by analyzing organic geochemistry characteristics: A case study of the Upper Triassic Yanchang Formation in the south of Ordos Basin, China [J]. Acta Geochim, 2016, 35(4): 1−13.

[31] YANDOKA B M S, ABUBAKAR M B, WAN H A, MAIGARI A S, HAKIMI M H, ADEGOKE A K, SHIRPUTDA J J, ALIYU A H. Sedimentology, geochemistry and paleoenvironmental reconstruction of the Cretaceous Yolde Formation from Yola Sub-basin, Northern Benue Trough, NE Nigeria [J]. Marine & Petroleum Geology, 2015, 67: 663−677.

[32] ROSENBERG M J, BIRGENHEIER L P, BERG M D V. Facies, stratigraphic architecture, and lake evolution of the oil shale bearing green river formation, Eastern Uinta Basin, Utah [M]. Stratigraphy and Paleolimnology of the Green River Formation, Western USA. Springer Netherlands, 2015: 211−249.

[33] DYNI J R. Geology and resources of some world oil-shale deposits [J]. Oil Shale, 2003, 3(20): 193−252.

[34] SONG Yu, LIU Zhao-jun, SUN Ping-chang, MENG Qing-tao, LIU Rong. A comparative geochemistry study of several oil shale-bearing intervals in the Paleogene Huadian Formation, Huadian Basin, northeast China [J]. Journal of Earth Science, 2017, 28(4): 1−11.

[35] PENG Xue-feng, WANG Li-jin, JIANG Li-ping. Geochemical characteristics of the lucaogou formation oil shale in the southeastern margin of the junggar basin and its environmental implications [J]. Bulletin of Mineralogy Petrology & Geochemistry, 2012, 2(31): 121−127. (in

Chinese)

[36] LIU Zhao-jun, MENG Qing-tao, DONG Qing-shui, ZHU Jian-wei, GUO Wei, YE Song-qing, LIU Rong, JIA Jian-liang. Characteristics and resource potential of oil shale in China [J]. Oil Shale, 2017, 34(1): 15−42.

[37] YANG Hua, NIU Xiao-bing, XU Li-ming, FENG Shen-bin, YOU Yuan, LIANG Xiao-wei, WANG Fang, ZHANG Dan-dan. Exploration potential of shale oil in Chang7 Member, Upper Triassic Yanchang Formation, Ordos Basin, NW China [J]. Petroleum Exploration and Development, 2016, 43(4): 511−520. (in Chinese)

[38] QIU Xin-wei, LIU Chi-yang, MAO Guang-zhou, DENG Yu, WANG Fei-fei, WANG Jian-qiang. Late Triassic tuff intervals in the Ordos basin, Central China: Their depositional, petrographic, geochemical characteristics and regional implications [J]. Journal of Asian Earth Sciences, 2014, 80:148−160.

[39] QIU X W, LIU C Y, WANG F F, DENG Y, MAO G Z. Trace and rare earth element geochemistry of the Upper Triassic mudstones in the southern Ordos Basin, Central China [J]. Geol J, 2015, 50: 399−413.

[40] LIU C Y, ZHAO H G, ZHAO J F, WANG J Q, ZHANG D D, YANG M H. Temporo-spatial coordinates of evolution of the ordos basin and its mineralization responses [J]. Acta Geologica Sinica, 2008, 82(6): 1229−1243.

[41] LI Wen-hou, PANG Jun-gang, CAO Hong-xia, XIAO Li, WANG Ruo-gu. Depositional system and paleogeographic evolution of the late Triassic Yanchang Stage in Ordos Basin [J]. Journal of Northwest University, 2009, 39(3): 501−506. (in Chinese with English abstract)

[42] ZOU C, WANG L, LI Y, TAO S, HOU L. Deep-lacustrine transformation of sandy debrites into turbidites, Upper Triassic, Central China [J]. Sedimentary Geology, 2012, 265−266(15): 143−155.

[43] WU Fu-tian, LI Wen-hou, LI Yu-hong, XI Sheng-li. Delta sediments and evolution of the Yanchang Formation of Upper Triassic in Ordos Basin [J]. Journal of Palaeogeography, 2004, 6(3): 307−315. (in Chinese)

[44] QIU Xin-wei, LIU Chi-yang, MAO guang-zhou, DENG Yu, WANG Fei-fei. Enrichment feature of thorium element in tuff Interlayers of upper Triassic Yanchang formation in Ordos basin [J]. Geological Bulletin of China, 2010, 29(8): 1185−1191. (in Chinese)

[45] DONG Li-hong, AN Si-jin, WANG Bian-yang. Relationship between distribution of hydrocarbon source rocks and oil-gas enrichment of yanchang formation, triassic, Ordos Basin [J]. Unconventional Oil & Gas, 2014(1): 17−21. (in Chinese)

[46] WANG Yong-dong, YAN Qi-bin. The resource application prospects of Zhangjiatan shale, Southern Ordos Basin [J]. Journal of Northwest University: Natural Science Edition, 2012, 42(3): 453−458. (in Chinese)

[47] HE Zi-xin. Evolution history and petroleum of the Ordos Basin [M]. Beijing: Petroleum Industry Press, 2003. (in Chinese)

[48] LI Rong-xi, XI Sheng-li, DI Ling-jun. Oil/gas reservoiring phases determined through petrographic analysis of hydrocarbon inclusions in reservoirs: Taking Longdong oilfield, Ordos basin, as an example [J]. Oil & Gas Geology, 2006, 27(2): 194−199. (in Chinese)

[49] GB/T14506.1-14-2010. Methods for chemical analysis of silicate rocks [S]. (in Chinese)

[50] GB/T14506.30-2010. Methods for chemical analysis of silicate Rocks-Part 30, Determination of 44 Elements [S]. (in Chinese)

[51] GB/T 18606-2001. The standard test method for biomarker in sediment and crude oil by GC-MS [S]. (in Chinese)

[52] SUGITANI K, YAMASHITA F, NAGAOKA T, YAMAMOTO K, MINAMI M, MIMURA K, SUZUKI K. Geochemistry and sedimentary petrology of archean clastic sedimentary rocks at mt. goldsworthy, pilbara craton, western australia: Evidence for the early evolution of continental crust and hydrothermal alteration [J]. Precambrian Research, 2006, 147(1, 2): 124−147.

[53] MIR A, BALARAM V, GANAI J, DAR S, KRISHNA K. Geochemistry of sedimentary rocks from Permian-Triassic boundary sections of Tethys Himalaya: Implications for paleo-weathering, provenance, and tectonic setting [J]. Acta Geochimica, 2016, 35(4): 428−436.

[54] CHEN Jian-fa, SUN Sheng-li. Preliminary study of geochemical characteristics and formation of organic matter rich stratigraphy of Xiamaling-Formation of later proterozoic in North China [J]. Nat Gas Geosci, 2004, 15(2): 110−114. (in Chinese)

[55] MCLENNAN S M. Relationships between the trace element composition of sedimentary rocks and upper continental crust [J]. Geochemistry Geophysics Geosystems, 2001, 2(4): 203−236

[56] SUN Sha-sha, YAO Yan-bin, LIN Wen. Elemental geochemical characteristics of the oil shale and the Paleo-Lake Environment of the Tongchuan Area, Southern Ordos Basin [J]. Bulletin of Mineralogy, Petrology and Geochemistry 2015, 34(3): 642−645. (in Chinese)

[57] CAO J, WU M, CHEN Y, HU K, BIAN L Z, WANG L G, ZHANG Y. Trace and rare earth element geochemistry of Jurassic mudstones in the northern Qaidam Basin, northwest China [J]. Chem Erde-Geochem, 2012, 72: 245−252.

[58] BAI Yue-yue, LIU Zhao-jun, SUN Ping-chang, LIU Rong, HU Xiao-feng, ZHAO Han-qing, XU Yin-bo. Rare earth and major element geochemistry of Eocene fine- grained sediments in oil shale- and coal-bearing layers of the Meihe Basin, Northeast China [J]. Journal of Asian Earth Sciences, 2015, 97(97): 89−101.

[59] HASKIN L A, HASKIN M A, FREY F A, WILDEMAN T R. Relative and absolute terrestrial abundances of the rare earths [J]. Origin and Distribution of the Elements, 1968: 889−912.

[60] TAYLOR S R, MCLENNAN S M. The geochemical evolution of the continental crust [J]. Reviews of Geophysics, 1985, 33(2): 241−265.

[61] ZHANG P, ZHENG J, ZHANG R, YU C. Rare earth elemental characteristics of ordovician-jurassic mudstone in Tabei Uplift, Tarim Basin [J]. Acta Sedimentologica Sinica, 2005, 23(4): 740−746.

[62] TU Qi-jun, XU Shi-qi. The REE Geochemistry of the Lucaogou formation in the southern Junggar basin and

analysis of parent rock and tectonic setting in sediment-source region [J]. Xinjiang Geology, 2016, 34(3): 345−349. (in Chinese)

[63] DUAN Yi, WU Bao-xiang, ZHUANG Hui, ZHENG Chao-yang, WANG Chuan-yuan. Geochemistry and Genesis of Crude oils of the Xifeng Oilfield in the Ordos Basin [J]. Acta Geologica Sinica, 2006(80): 301−310. (in Chinese)

[64] DUAN Yi, YU Wen-xiu, LIU xian-yang, GUO Zheng-quan, WU Bao-xiang, SUN Tao, WANG Chuan-yuan. Oil migration and accumulation rules of Chang9 oil-bearing formation in the Ordos Basin [J]. Acta Geologica Sinica, 2009(83): 855−860. (in Chinese)

[65] DUAN Y, YUAN Y, QIAN R. Migration features of crude oil in fluvial deposits of Maling oilfield in Ordos Basin, China [J]. Organic Geochemistry, 2013, 58: 78−85.

[66] MA Yu, ZHOU Shi-xin, TAO Hui-fei, FU De-liang, LI Jing, LI Yuan-ju, LI Cheng-cheng, YANG Ya-nan. Sedimentary characteristic and organic matter enrichment factors of the Chang-7 section shale of Yanchang Formation in the south of Ordos Basin [J]. Chinese Journal of Geology, 2017, 52(1): 106−122. (in Chinese)

[67] WU Kai, ZHANG Wen-zheng, CHEN Fang, LI Shan-peng, KONG Qing-fen, SUN Lin. Organic geochemical characteristics of organic-matter-rich oil shale in the Yanchang formation Chang 7 reservoirs of Gucheng Area, Ordos Basin [J]. Low Permeability Oil & Gas Fields, 2008(3): 5−10. (in Chinese)

[68] ER chuang, LI Yang-yang, ZHAO Jing-zhou, WANG Rui, WEI Zhi-kun. Lithofacies features of organic-rich shale of the Triassic Yanchang Formation in Huachi Aera, Ordos Basin [J]. Earth Science Frontiers, 2016, 23(2): 108−117. (in Chinese)

[69] LIN S, YUAN X, TAO S, YANG Z, WU S T. Geochemical Characteristics of the source rocks in Mesozoic Yanchang formation, central Ordos Basin [J]. Journal of Earth Science, 2013, 24(5): 804−814.

[70] YUAN Xuan-jun, LIN Sen-hu, LIU Qun, YAO Jing-li, WANG Lan, GUO Hao, DENG Xiu-qin, CHENG Da-wei. Lacustrine fine-grained sedimentary features and organic-rich shale distribution pattern: A case study of Chang 7 Member of Triassic Yanchang Formation in Ordos Basin, NW China [J]. Petroleum Exploration and Development, 2015, 42(1): 34−43. (in Chinese)

[71] MEI B. The distribution of isoprenoid alkanes in China’s crude oil and its relation with the geologic environment [J]. Oil & Gas Geology, 1980(1): 99−115. (in Chinese)

[72] HUANG D, LI J, ZHANG D. Maturation sequence of continental crude oils in hydrocarbon basins in China and its significance [J]. Organic Geochemistry, 1990, 16: 521−529.

[73] SEIFERT W K, MOLDOWAN J M. Use of biological markers in petroleum exploration [J]. Methods in Geochemistry & Geophysics, 1986, 24: 261−290.

[74] ERNST T W. Geochemical Facies Analysis [M]. Amsterdam: Elsevier, 1970.

[75] DYPVIK H, HARRIS N B. Geochemical facies analysis of fine grained siliciclastics using Th/U, Zr/Rb and (Zr+Rb)/Sr ratios [J]. Chemical Geology, 2001, 181: 131−146.

[76] JONES B, MANNING D A C. Comparison of geochemical indices used for the interpretation of depositional environments in ancient mudstones [J]. Chemical Geology, 1994, 111(1−4): 112−129.

[77] TRIBOVILLARD N, ALGEO T J, LYONS T, RIBOULLEAU A. Trace metals as paleoredox and paleoproductivity proxies−An update [J]. Chemical Geology, 2006, 232(1, 2): 12−32.

[78] ZHAO Bang-sheng, LI Rong-xi, WANG Xiang-zeng, WU Xian-yang, WANG Ning, QIN Xiao-li, CHENG Jing-hua, LI Jia-jia. Sedimentary environment and preservation conditions of organic matter analysis of shanxi formation mud shale in Yanchang Exporation Area, Ordos Basin [J]. Geological Science And Technology Information, 2016, 35(6): 103−111. (in Chinese)

[79] TENG ge-er, LIU Wen-hui, XU Yong-chang,CHENG Jia-fa. Correlative study on parameters of inorganic geochemistry and hydrocarbon source rocks formative environment [J]. Advance in Earth Sciences, 2005, 20(2): 193−200. (in Chinese)

[80] ZHANG Wen-zheng, YANG Hua, XIE Li-qin, XIE Gu-wei. Discovery of micro- and Nano-fossils in high grade hydrocarbon source rocks of the Triassic Yanchang formation Chang 7 member in ordos basin and its scientific significance [J]. Acta Palaeontologica Sinica, 2011(1): 109−117. (in Chinese)

[81] LIU Xing-jun, LIU Yi-qun, ZHOU Ding-wu, LIU Hong, ChENG Xin-hu, NAN Yun. Deep fluid tracer in Ordos Basin: Characteristics and origin of high natural gamma sandstone in Triassic Yanchang Formation [J]. Earth Science Frontiers, 2013, 20(5): 149−165. (in Chinese)

[82] CHU Cheng-lin, CHEN Qiang-lu, ZHANG Bo, SHI Zheng, JIANG Hai-jian, YANG Xin. Influence on formation of Yuertusi source rock by hydrothermal activities at Dongergou Section, Tarim Basin [J]. Acta Sedimentologica Sinica, 2016, 34(4): 803−810. (in Chinese)

[83] HE C, JI L, WU Y, WU Y, AO S, ZHANG M. Characteristics of hydrothermal sedimentation process in the Yanchang Formation, South Ordos Basin, China: Evidence from element geochemistry [J]. Sedimentary Geology, 2016, 345: 33−41.

[84] LI Shuang-jian, XIAO Kai-hua, WO Yu-jun, LONG Sheng-xiang, CAI Li-guo. REE geochemical characteristics and their geological signification in silurian, West of Hunan province and north of Guizhou province [J]. Geoscience, 2008, 22(2): 273−280. (in Chinese)

[85] YANG Wan-qin, JIANG You-lu, WANG Yong. Study on shale facies sedimentary environment of lower Es_3-upper Es_4 in Dongying sag [J]. Journal of China University of Petroleum: Edition of Natural Science, 2015, 39(4): 19−26. (in Chinese)

[86] WAN Jin-feng, XIAN Ben-zhong, SHE Yuan-qi, YANG Li-qiang. Palaeobathymetric reconstruction based on natural gamma ray spectrometry logging data-by taking Bachu formation in region 4 of Tahe oilfield for example [J]. Journal of Oil And Gas Technology, 2011, 33(6): 98−103. (in Chinese)

[87] WAN Y S, XIE H Q, YANG H, WANG A J, LIU D Y, KRÖNER A, WILDE S A, GENG Y S, SUN L Y, MA M Z, LIU S J, DONG C Y, DU L L. Is the ordos block archean or paleoproterozoic in age? Implications for the Precambrian evolution of the North China craton [J]. American Journal of Science, 2003, 313: 683−711.

[88] YANG R, FAN A, HAN Z, LOON A J V. Lithofacies and origin of the late triassic muddy gravity-flow deposits in the Ordos Basin, central China [J]. Marine & Petroleum Geology, 2017, 85: 194−219.

(Edited by FANG Jing-hua)

中文导读

鄂尔多斯盆地南部三叠系油页岩沉积条件及沉积模型

摘要：基于主量元素、微量元素、稀土元素和生物标志化合物等测试，探讨鄂尔多斯盆地南部三叠系延长组长 7 油页岩的沉积环境和有机质来源。样品的甾烷特征表明油页岩具有相似的有机质来源，以藻类生物和高等植物为主。U/Th 和 V/Ni 比值表明油页岩沉积于还原环境，铜川地区的缺氧程度较高。Sr/Ba 比值表明油页岩沉积在淡水环境中，但铜川地区的盐度高于旬邑地区。Fe/Ti 比值表明铜川地区经历了明显的热流体活动。Sr/Cu 比值表明两个地区沉积期古气候均为温湿气候，没有明显差异。$(La/Yb)_{NASC}$ 表明铜川地区沉积速率低于旬邑地区。Fe/Co 和 Th/U 比值均表明铜川地区的古水体较旬邑地区深。有机质来源分析结果表明，水体中有机质既有低等藻生生物也有高等植物来源，推测这和秦岭造山运动有关。综合对比上述古沉积环境，认为相比于旬邑地区，铜川地区是鄂尔多斯盆地南部三叠系油页岩勘探的重点区域。

关键词：油页岩；地球化学；沉积模型；长 7；鄂尔多斯盆地